energies

MDPI

Article

A Slime Mould Algorithm Programming for Solving Single and Multi-Objective Optimal Power Flow Problems with Pareto Front Approach: A Case Study of the Iraqi Super Grid High Voltage

Murtadha Al-Kaabi [1,2,*], Virgil Dumbrava [1] and Mircea Eremia [1]

[1] Department of Power Systems, Faculty of Energy, University Politehnica of Bucharest, 060029 Bucharest, Romania
[2] School Buildings Department, Ministry of Education, Rusafa 3, Baghdad 10059, Iraq
* Correspondence: mmsk.1986s@gmail.com; Tel.: +964-7500580065

Abstract: Optimal power flow (OPF) represents one of the most important issues in the electrical power system for energy management, planning, and operation via finding optimal control variables with satisfying the equality and inequality constraints. Several optimization methods have been proposed to solve OPF problems, but there is still a need to achieve optimum performance. A Slime Mould Algorithm (SMA) is one of the new stochastic optimization methods inspired by the behaviour of the oscillation mode of slime mould in nature. The proposed algorithm is characterized as easy, simple, efficient, avoiding stagnation in the local optima and moving toward the optimal solution. Different frameworks have been applied to achieve single and conflicting multi-objective functions simultaneously (Bi, Tri, Quad, and Quinta objective functions) for solving OPF problems. These objective functions are total fuel cost of generation units, real power loss on transmission lines, total emission issued by fossil-fuelled thermal units, voltage deviation at load bus, and voltage stability index of the whole system. The proposed algorithm SMA has been developed by incorporating it with Pareto concept optimization to generate a new approach, named the Multi-Objective Slime Mould Algorithm (MOSMS), to solve multi-objective optimal power flow (MOOPF) problems. Fuzzy set theory and crowding distance are the proposed strategies to obtain the best compromise solution and rank and reduce a set of non-dominated solutions, respectively. To investigate the performance of the proposed algorithm, two standard IEEE test systems (IEEE 30 bus IEEE 57 bus systems) and a practical system (Iraqi Super Grid High Voltage 400 kV) were tested with 29 case studies based on MATLAB software. The optimal results obtained by the proposed approach (SMA) were compared with other algorithms mentioned in the literature. These results confirm the ability of SMA to provide better solutions to achieve the optimal control variables.

Keywords: optimal power flow; single- and multi-objective functions; slime mould algorithm; pareto concept; generation fuel cost; real power losses; voltage stability index; voltage deviation; emission

Citation: Al-Kaabi, M.; Dumbrava, V.; Eremia, M. A Slime Mould Algorithm Programming for Solving Single and Multi-Objective Optimal Power Flow Problems with Pareto Front Approach: A Case Study of the Iraqi Super Grid High Voltage. *Energies* **2022**, *15*, 7473. https://doi.org/10.3390/en15207473

Academic Editors: Ragab A. El-Sehiemy, Attia El-Fergany and Almoataz Youssef Abdelaziz

Received: 23 August 2022
Accepted: 8 October 2022
Published: 11 October 2022

1. Introduction

Power flow (PF), also known as load flow, is one of fundamental issues in electrical power systems. The main idea of power flow analysis is to find out the reactive power output in transmission lines, the voltage at buses, and total losses in the whole system at operation conditions. In recent decades, optimal power flow (OPF) has been given extensive interest by researchers because it is one of the most important tools used in power management systems to achieve the reliable operation and planning of electrical power systems [1]. To optimize objective functions in the power system, OPF needs to set the control variables while respecting equality and inequality constraints because OPF is a non-convex, nonlinear, and large-scale problem. The active power output of the generation units without the slack bus, the voltages at PV buses, reactive power compensators, and tap transformers settings are the control variables that are tuned. The generation fuel cost

(GFC), real power loss (RPL) in the transmission lines, emission (Em), voltage deviation (VD), and voltage stability index (VSI) in the whole system are the objective functions that will be optimized. OPF was first presented by Carpentier in 1962 [2].

Two types of optimization methods that have been proposed to solve OPF problems are classical and intelligent optimization methods. Several classical methods have been applied, such as linear and nonlinear programming, interior point method, the Newton method, quadratic programming, and mixed-integer programming [3,4]. Although these techniques provide an optimal solution, their drawbacks cannot reach a local minimum if it is assumed that the initial point is not close to the solution. Further, the quality of solutions is inversely proportional to a number of control variables. In addition, due to increasing the number of non-linear constraints, the problems are more complex. The second type of optimization algorithms is intelligent optimization techniques, such as grey wolf optimizer (GWO) [5], hunger games search (HGS) [6], Harris hawks optimization [7], Nomadic People Optimizer [8], and the honey badger algorithm (HBA) [9].

A Slime Mould Algorithm (SMA) is one of new optimization algorithms that has been proposed to solve the OPF problem in the power system. SMA is a meta-heuristic algorithm inspired by the diffusion and foraging conduct of slime mould proposed in 2020 by S. Li et al. [10]. SMA has many features, such as:

(i) The mathematical model used in this algorithm is unique. It uses adaptive weights, which are allowed to produce positive and negative feedback in the simulation process for propagation wave.
(ii) The form path of connection food is optimal using a bio-oscillator.
(iii) The ability and propensity for exploration and exploitation is excellent.

Several articles have solved single-objective OPF problems using intelligent optimization techniques, such as differential evolution (DE) [11], modified artificial bee colony (MABC) [12], improved differential evolution (IDE) [13,14], Harris hawks optimization [15], and the moth swarm algorithm (MSA) [16]. On the other hand, several approaches have been proposed to solve multi-objective optimization (MOO), such as a weighted sum [17], the penalty function method [18], ε-constant [19], the non-dominated sorting genetic algorithm-based approach [20], and the strength Pareto evolutionary algorithm [21]. The most popular method used to solve multi-objective optimization (MOO) problems is Pareto optimization (PO) [22]. One of the main features of this method is a comparison of conflicting objective functions (OFs) to choose favourable solutions [23]. The fuzzy membership approach is the approach taken in the decision-making process to select the best compromise solution in the Pareto front computations.

Multi-objective optimal power flow (MOOPF) is most important in power systems operation and planning because of its ability to find the best compromise solution for more than one objective function simultaneously [24]. The Pareto concept is incorporated with many optimization methods to arrange the non-dominated solutions and set the generation probability for individuals. Many optimization algorithms have been proposed to solve MOOPF in electrical power system, such as the Multi-Objective Improved Differential Evolution Algorithm (MOIDEA) [25], multi-objective backtracking search algorithm (MOBSA) [26], Jaya Optimization [27], Multi-Objective Manta Ray Foraging Optimizer (MOMRFO) [28], Multi-Objective Ant Lion Optimizer (MOALO) [29], and Harris Hawks Optimization (HHO) [30].

In this paper, a newly proposed algorithm (proposed in 2021), named the Slime Mould Algorithm (SMA), is suggested to solve a single-objective function on three systems: IEEE 30 bus and IEEE 57 bus test systems, and one practical system (Iraqi Super Grid High voltage 400 kV). In addition, the proposed algorithm SMA was developed by incorporating it with Pareto concept optimization to generate a new approach, named the Multi-Objective Slime Mould Algorithm (MOSMS), to solve multi-objective (Bi, Tri, Quad, and Quinta) optimal power flow problems. The approach used to extract best compromise solution is fuzzy set theory. Generation fuel cost (GFC), emission (Em), real power losses (RPL),

voltage deviation (VD), and voltage stability index (VSI) are the objective functions that will be optimized. It can be summarized the main contribution as follows:

1. The Slime Mould Algorithm was developed to solve single- and multi-objective optimal power flow to achieve the economic, environmental, and technical benefits of power systems.
2. The Pareto concept is the approach taken to rank store non-dominated Pareto fronts, crowding distance is the mechanism to reduce the Pareto repository, and fuzzy set theory is the theory applied to extract the best compromise solution.
3. Two standard IEEE test systems (IEEE 30 bus IEEE 57 bus systems) and a one practical network (Iraqi Super Grid High Voltage 400 kV) were applied with 29 case studies for single- and multi-objective (Bi, Triple, Quad, and Quinta) functions.
4. The optimal results obtained by the proposed algorithm were compared with other recent optimization methods in the literature.

The remainder of this paper can be summarized as follows: Section 2 present the OPF problem formulation, including the general OPF formulation, objective functions, and operational constraints. Section 3 is the mathematical model of Slime Mould Algorithm (SMA). Section 4 introduce the strategy taken in multi-objective solutions. Section 5 discussed the numerical results for 29 cases and compared them with other recent optimization methods. Finally, the conclusions are presented in Section 6.

2. OPF Problem Formulation

In power systems, the objective functions can be optimized by set control variables as optimally with satisfied the equality and inequality constraints. The mathematical model of OPF problems can be described by the following:

$$\begin{array}{lll} \text{Optimize} & f(x,u) & \\ \text{subjected to} & \mathrm{g}_i(x,u)=0 & i=1,2,\ldots,\mathrm{m} \\ & h_i(x,u)\le 0 & i=1,2,\ldots,\mathrm{p} \end{array} \tag{1}$$

These vectors can be symbolized as:

$$x=\left[P_{G_1},|\mathrm{V}_{L_1}|,\cdots,\left|V_{L_{PQ}}\right|,Q_{G_1}\cdots Q_{G_{PV}}\right] \tag{2}$$

$$u=\left[P_{G_2},\cdots,P_{G_{PV}},|V_{G_1}|,\cdots,|V_{G_{PV}}|,T_1,\cdots,T_{NT},Q_{C_1},\cdots,Q_{C_{NC}}\right] \tag{3}$$

2.1. Objective Functions

The objective functions will be optimized are generation fuel cost (GFC), real power losses (RPL), emission (Em), voltage deviation (VD), and voltage stability index (VSI).

1. Generation Fuel Cost (GFC) (USD/h)

The mathematical formula that has been described to GFC is [31]:

$$F_{GFC}=\sum_{i=1}^{N_G}\left(a_iP_{G_i}^2+b_iP_{G_i}+c_i\right)\quad (USD/h) \tag{4}$$

2. Real Power Losses (RPL) (MW)

The mathematical formula that has been described to GFC is [31]:

$$F_{RPL}=\sum_{k=1}^{N_{nl}}G_{(i,j)}\left(V_i^2+V_j^2-2V_iV_j\cos\delta_{i,j}\right)\quad (MW) \tag{5}$$

3. Emission (Em) (ton/h)

Emission (Em) can be expressed of the mathematical description of greenhouse gases emissions, such as NOx and SOx, as follows:

$$F_{Em} = \sum_{i=1}^{N_G} 10^{-2}\left(\alpha_i + \beta_i P_{G_i} + \gamma_i P_{G_i}^2\right) + \zeta_i \exp\left(\lambda_i P_{G_i}\right) \quad (ton/h) \tag{6}$$

4. Voltage Deviation (VD) (p.u.)

The voltage level at buses is a very important factor to achieve stability and economic benefits by keeping the voltages of each bus close to the reference voltage. The formula that expressed of voltage deviation is given by [32]:

$$F_{VD} = \sum_{i=1}^{N_{PQ}} \left|V_i - V_{ref}\right| \quad (p.u.) \tag{7}$$

Here, V_{ref} denotes the rated voltage magnitude, which the value is 1.0 (p.u.).

5. Voltage Stability Index (VSI)

The maximum value of the voltage stability indicator (L-index) will be minimized by enhancing the voltage stability of the whole system. The following equation represents the mathematical formula of VSI [32]:

$$F_{VSI} = Max\left(L_j\right) \tag{8}$$

$$L_j = \left|1 - \sum_{i=1}^{N_G}\left(F_{ji} \times \frac{V_i}{V_j}\right)\right| \tag{9}$$

$$F_{ji} = -[Y_{LL}]^{-1} \times [Y_{LG}] \tag{10}$$

2.2. Constraints

In OPF, equality constraints (active and reactive powers) represent the physical structure of the whole system. It can be expressed as [33]:

$$P_{gi} - P_{di} = |V_i| \sum_{j=1}^{N} \left|V_j\right| \left(g_{ij} \cos \delta_{ij} + b_{ij} \sin \delta_{ij}\right) \qquad \forall i \in N \tag{11}$$

$$Q_{gi} + Q_{ci} - Q_{di} = |V_i| \sum_{j=1}^{N} \left|V_j\right| \left(g_{ij} \sin \delta_{ij} - b_{ij} \cos \delta_{ij}\right) \quad \forall i \in N \tag{12}$$

The other constraints are inequality constraints (generator, transformer, shunt compensator, and security). These constraints represent the operation limit to achieve the stable operation of the system. It can be described as follows [33]:

1. Generator Constraints:

$$P_{gi}{}^{\min} \le P_{gi} \le P_{gi}{}^{\max} \qquad i = 1, 2, \ldots, N_g \tag{13}$$

$$Q_{gi}{}^{\min} \le Q_{gi} \le Q_{gi}{}^{\max} \qquad i = 1, 2, \ldots, N_g \tag{14}$$

$$V_{gi}{}^{\min} \le V_{gi} \le V_{gi}{}^{\max} \qquad i = 1, 2, \ldots, N_g \tag{15}$$

2. Shunt Compensator Constraints:

$$Q_{c_k}{}^{\min} \le Q_{c_k} \le Q_{c_k}{}^{\max} \qquad k = 1, 2, \ldots, N_c \tag{16}$$

3. Transformer Constraints:

$$T_j^{\min} \le T_j \le T_j^{\max} \qquad j = 1, 2, \ldots, N_T \tag{17}$$

4. Security Constraints:

$$V_{Li}^{\min} \le V_{Li} \le V_{Li}^{\max} \qquad i = 1, 2, \ldots, N_L \tag{18}$$

$$S_{L_m} \le S_{L_m}^{\max} \qquad m = 1, 2, \ldots, N_{nl} \tag{19}$$

3. The Mathematical Model of the Slime Mould Algorithm (SMA)

The Slime Mould Algorithm (SMA) is a new optimization algorithm inspired by the diffusion and behaviour conduct of slime mould in nature and proposed by S. Li et al. in 2021 [10]. The processes of SMA by approaching food, wrapping food, and oscillating can be summarized as follows:

3.1. Approach Food

The approaching behaviour can be expressed as mathematical formulae as follows:

$$Y(t+1) = \begin{cases} Y_b(t) \cdot ub \cdot (V \cdot Y_A(t) - Y_B(t)), & r < p \\ uc \cdot Y(t), & r \ge p \end{cases} \tag{20}$$

The formula of p is as follows [10]:

$$p = \tanh(|fit(i) - df|) \tag{21}$$

where $i \in 1,2, \ldots, n$. It can be expressed as follows:

$$a = \operatorname{arctanh}\left(-\left(\frac{t}{t\_\max}\right) + 1\right) \tag{22}$$

The formula of V is as follows:

$$W(\mathrm{SmIndex}(i)) = \begin{cases} 1 + r \cdot \log\left(\frac{bf - R(i)}{bf - wf} + 1\right), & condition \\ 1 - r \cdot \log\left(\frac{bf - R(i)}{bf - wf} + 1\right), & other \end{cases} \tag{23}$$

$$\mathrm{SmIndex} = \mathrm{sort}(\mathrm{R}) \tag{24}$$

3.2. Wrap Food

To update the slime mould location, the mathematical formula can be expressed as:

$$Y = \begin{cases} rand \cdot (ub - lb) + lb, & rand < z \\ Y_b(t) + ub \cdot (V \cdot Y_A(t) - Y_B(t)), & r < p \\ uc \cdot Y(t), & r \ge p \end{cases} \tag{25}$$

3.3. Oscillation

The variations of slime mould will be simulated to find the food by the parameters V, ub, and uc. To select the best food source, the slime mould should be improved by the oscillation frequency, which is mathematically expressed by V. The velocity of slime mould to discover food depends on the concentration of food. If the concentration of food is high, then the velocity of slime mould will be faster, but the velocity of slime mould will be slow if the concentration of food is low. ub oscillates in the interval $[-a, a]$ as randomly and decreased to zero when the iteration is increased. In addition, uc oscillates in the range $[-1, 1]$ and gradually decreases to zero when the iteration increases. The flowchart and Pseudo-code of SMA are expressed in Figure 1 and Algorithm 1.

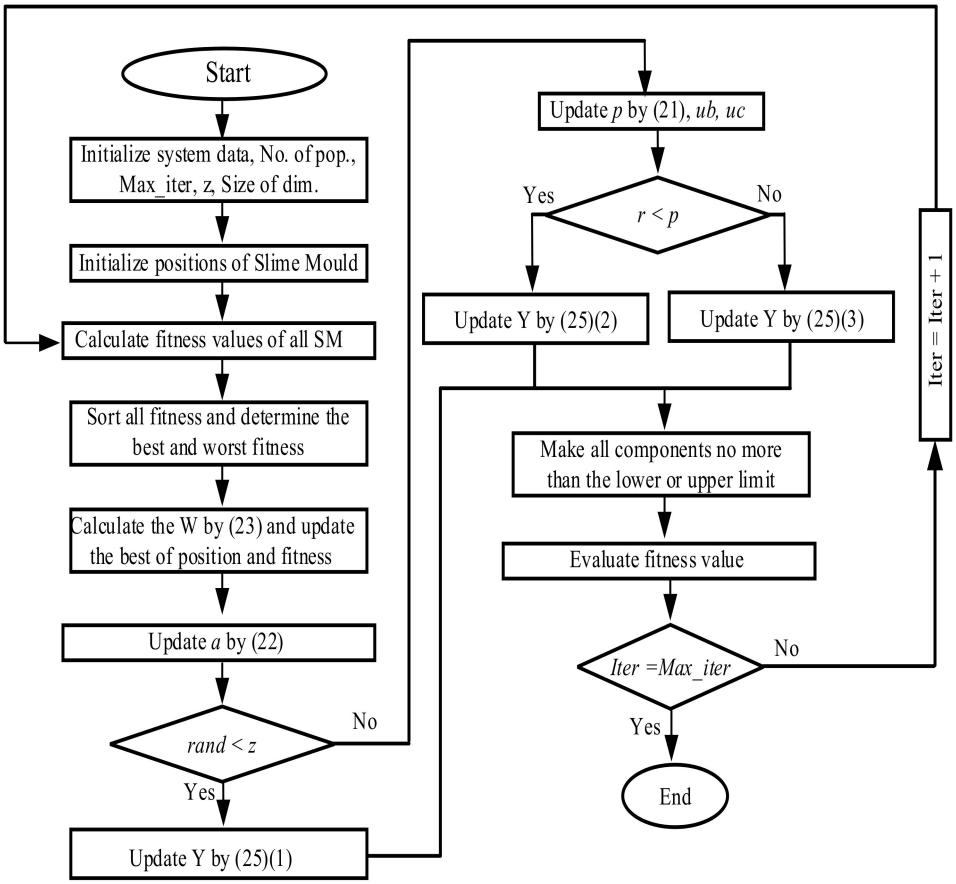

Figure 1. Flowchart of the SMA.

Algorithm 1. Pseudo-code of the Slime Mould Algorithm (SMA)

```
Select the values of parameters pop_size, Max_t
Determine the positions of slime mode Y_i (i = 1, 2, ..., N)
While (t ≤ Max_t)
    Calculate R(i) of all slime mode
    Update bf, Y_b
    Calculate W Equation (23)
    For each search portion
      Update p, ub, uc
      Update positions by Equation (25)
    End (For)
    t = t + 1
End (While)
Return bf, Y_b
```

4. Multi-Objective Slime Mould Algorithm (MOSMA)

The main purpose of using multi-objective optimization is to optimize two or more objectives simultaneously (mostly conflicting and non-commensurable objectives) in power systems. In MOSMA, the concept used for classification the dominated and non-dominated solutions, based on objective functions, is Pareto dominance. The fuzzy decision-maker is the strategy taken to extract the best compromise solution.

4.1. Pareto Optimization Approach

The Pareto optimization approach can solve the problems related to single-objective optimization directly. Therefore, it is much more difficult to determine a suitable solution for problems related to multi-objective optimization. One of the popular solutions to solve

multi-objective optimization problems is simplified into single-objective optimization by determining the different weights of each objective and summing these objectives. Due to the conflicting objective functions, it is not easy to determine the optimal solution to multi-objective optimization problems. In other words, if a solution is not superior to other solutions based on the objective function, the solution is not dominated, then these solutions are called the non-dominated solutions. The Pareto dominates solutions achieved when:

$$\begin{array}{l} \forall i \in \{1, 2, \ldots, n\} : F_i(X_1) \leq F_i(X_2) \\ \exists j \in \{1, 2, \ldots, n\} : F_j(X_1) < F_j(X_2) \end{array} \tag{26}$$

where $F_i(X_1)$ and $F_i(X_2)$ are the *ith* objective function values of solutions X_1 and X_2. Based on Equation (26), the solution X_1 should be dominated solution X_2 to satisfy Pareto front non-dominated solutions. In Pareto concept optimization, the fitness of objective function will be compared with each other for all solutions. The dominated solutions are achieved when the fitness of objective function for a solution is higher than the fitness of objective function of any other solutions. On the contrary, the obtained solutions called dominated solutions. The main aim of Pareto concept optimization is to obtain the set of non-dominated solutions of multi-objective optimization problems. Therefore, the solutions obtained by Pareto optimization do not represent the optimal solution of each objective function. The Pareto fronts non-dominated (PFND) solutions represent a set of non-dominated solutions that are plotted as curve in the solutions space.

The set of solutions that could not dominate each other are called Pareto optimal solutions. These sets will be continuously updated and stored to solve multi-objective problems.

4.2. Best Compromise Solution

It necessary to unify the values of objective function in a similar range because there are different ranges. The incompatibility with the sets can be indicated as value 0, while the full compatibility indicated as value 0, as shown in Figure 2. Each objective function has a membership function as follows:

$$u_i^k = \begin{cases} 1 & F_i \leq F_i^{\min} \\ \frac{F_i^{\max} - F_i}{F_i^{\max} - F_i^{\min}} & F_i^{\min} < F_i < F_i^{\max} \\ 0 & F_i \geq F_i^{\max} \end{cases} \tag{27}$$

$$u_i^k = \frac{\sum_{i=1}^{N_{obj}} u_i^k}{\sum_{k=1}^{M} \sum_{i=1}^{N_{obj}} u_i^k} \tag{28}$$

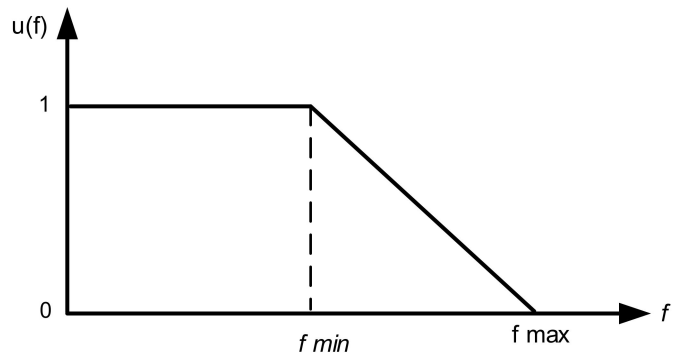

Figure 2. Membership function.

The maximum value of u^k represents the best compromise solution [27].

4.3. Phases of MOSMA

The stages of MOSMA can be summarized as follows:

Step 1: Initialize the main parameters, such as the no. of population, no. of control variables, no. of non-dominated solutions, max iterations, etc . . .

Step 2: Initialize the population of slime mould.

Step 3: Calculate the fitness function of each individual of the initial population.

Step 4: Sort the initial population according on the fitness function of each individual and save the non-dominated solutions into initial repository.

Step 5: Calculate the best and the worst compromise solution of the initial population according to Equation (28).

Step 6: Calculate the weight of slime mould of non- dominant solutions by (24).

Step 7: Calculate the parameter *a* by (22).

Step 8: Update the position of slime mould according to (25).

Step 9: Update the position of the slime mould to be within lower or upper bounds.

Step 10: Calculate the fitness value of each slime mould position.

Step 11: Sort the non-dominated solutions of slime mould position and store them in the slime mould repository.

Step 12: Combined the non-dominated solutions in the initial repository with the non-dominated solutions in the slime mould repository to find new non-dominated solutions.

Step 13: Verify the stopping criteria and check if the new non-dominated solutions are equal to or more than the number of non-dominated that have been suggested. If this is the case, then the program will end. Otherwise, store the new non-dominated solutions as in the initial repository and return to Step 5.

The process of the multi-objective slime mould algorithm (MOSMA) to solve multi-objective optimal power flow can be described in the flowchart in Figure 3

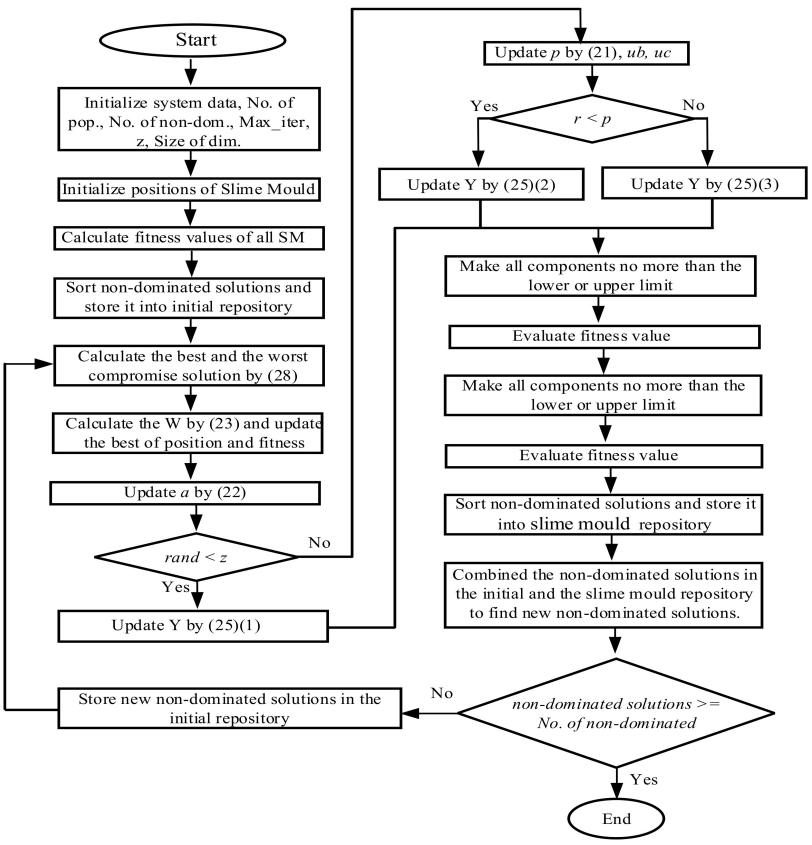

Figure 3. Flowchart of MOSMA.

4.4. Crowding Distance

A crowding distance is a strategy used to reduce the non-dominate solutions by calculating the average distance for two neighbouring solutions. First, the fitness value of the objective function must be sorted in ascending order depending on the nearest neighbours. Then, the fitness values of the boundary solutions are evaluated as the infinite distance value. The fitness value of the intermediate solutions is equal to the distance of the corresponding diagonal length. Figure 4 represents the diagonal length of the cuboid to calculate the crowding distance. It is expressed as follows:

$$CD_i = \prod_{n=1}^{m} \frac{|F_n(X_i + 1) - F_n(X_i - 1)|}{F_{n,\min}}, \qquad i = 1, 2, \cdots, N_b \tag{29}$$

where CD_i denotes the crowding distance, $F_{n,\,min}$ represents the minimum value of nth objective function, and N_b is the number of candidate solutions.

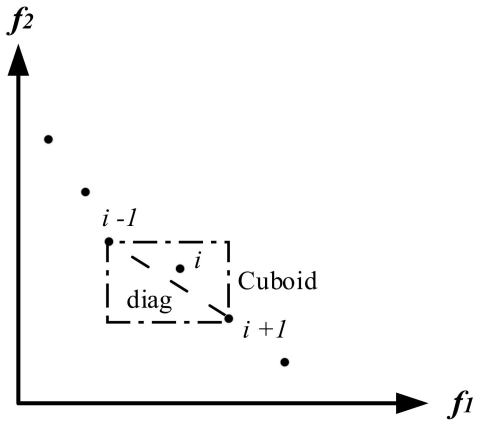

Figure 4. The estimation of crowding distance.

5. Simulation Results

To demonstrate the effectiveness and performance of SMA to solve OPF problems, two standard systems (IEEE-30 bus system and IEEE 57-bus test system) and one practical system (Iraqi Super Grid High Voltage ISGHV 400 kV) were used to test with 29 cases for various objective functions. The characteristics of these systems are presented in Table 1. Table 2 describes the studies that have been applied.

Table 1. The main characteristics of the systems applied in this study.

System Characteristics	IEEE-30	IEEE 57	ISGHV 400 kV
Buses	30	57	28
Branches	41	80	44
Generators	9 (Buses:1, 2, 5, 8, 11 and 13)	7 (Buses: 1–2–3–6–8–9–12)	14 (Buses: 1–14)
Generator voltage limits	0.9–1.1 [p.u.]	0.9–1.1 [p.u.]	0.9–1.1 [p.u.]
Load voltage limits	0.95–1.05 [p.u.]	0.95–1.05 [p.u.]	0.95–1.05 [p.u.]
Limit of tap changer setting	0.9–1.1 [p.u.]	0.9–1.1 [p.u.]	-
Limit of VAR	0–5 [p.u.]	0–20 [p.u.]	-
Shunts	9 (Buses: 10, 12, 15, 17, 20, 21, 23, 24 and 29)	3 (Buses: 18–25–53)	-
Transformers	4 (Buses: 11, 12, 15 and 36)	17 (Buses: 19–20–31–35–36–37–41–46–54–58–59–65–66–71–73–76–80)	-
MW demand	283.4 [MW]	1250.8 [MW]	5994 [MW]
Control variables	24	33	27

Table 2. Various case studies.

Type of System	Type of OF(s)	Case #	FC	Em	RPL	VD	VSI
IEEE 30-bus	Single OF(s)	Case #1	√				
		Case #2			√		
		Case #3		√			
		Case #4				√	
		Case #5					√
	Bi-OF(s)	Case #6	√	√			
		Case #7	√		√		
		Case #8	√		√		
		Case #9	√				√
		Case #10		√		√	
		Case #11			√	√	
		Case #12				√	√
	Triple-OF(s)	Case #13	√	√	√		
		Case #14	√	√		√	
		Case #15	√		√	√	
		Case #16	√		√		√
		Case #17	√	√			√
		Case #18	√			√	√
		Case #19		√	√	√	
	Quad-OF(s)	Case #20	√	√	√	√	
		Case #21	√	√	√		√
	Quinta-OF(s)	Case #22	√	√	√	√	√
IEEE 57-bus	Single OF(s)	Case #23	√				
		Case #24			√		
		Case #25		√			
ISGHV 400 kV (28 bus)	Single OF(s)	Case #26	√				
		Case #27			√		
		Case #28				√	
		Case #29					√

5.1. IEEE 30-Bus Power System

The data of the IEEE 30 bus system are given in [34]. The main characteristics of IEEE 30-bus power system are given in Table 1. The coefficients of cost and emission of generators are given in Table A1. Figure A1 represents the single-line diagram of the IEEE 30 bus test system.

5.1.1. Single-Objective OPF on IEEE 30-Bus Power System

Five objective functions were optimized to solve OPF problem— the generational fuel cost (GFC), real power loss (RPL), emission (Em), voltage deviation (VD), and voltage stability index (VSI)—by setting the parameters of the control variables (active power output of generators except for the slack bus, the voltage of PV bus, tap ratio of transformers, and shunt VAR compensator). In total, 1000 iterations and 250 population sizes were the values chosen in SMA to solve OPF problem. The finest settings of optimal control variables to find the optimal objective function for five cases are reported in Table 3.

Table 3. Optimal control variables obtained by SMA for Cases 1–5.

Item		Limit		Initial [35]	Case 1	Case 2	Case 3	Case 4	Case 5
		Max	Min						
P_g [MW]	P_1	50	200	99.223	176.9638	52.66583	67.23830	122.9787	153.8864
	P_2	20	80	80	48.54495	79.60434	71.62589	45.29825	23.85954
	P_5	15	50	50	21.21892	49.92812	49.99828	47.87340	36.47932
	P_8	10	35	20	21.38800	34.60913	34.97310	29.73724	34.96892
	P_{11}	10	30	20	11.92001	29.92682	29.99790	21.98221	20.91042
	P_{13}	12	40	20	12.02793	39.65335	33.16002	21.74010	19.63984
V_g [p.u.]	V_1	0.95	1.1	1.05	1.09999	1.09997	1.07207	0.99759	1.09925
	V_2	0.95	1.1	1.04	1.09786	1.09672	1.09211	0.98059	1.09803
	V_5	0.95	1.1	1.01	1.08201	1.09541	1.03596	1.06050	1.08448
	V_8	0.95	1.1	1.01	1.08952	1.08871	1.04344	1.04797	1.08762
	V_{11}	0.95	1.1	1.05	1.09966	1.09989	1.08511	1.09352	1.09901
	V_{13}	0.95	1.1	1.05	1.09959	1.09955	1.04750	1.06366	1.09924
Shunt Element [MVAr]	Q_{c10}	0	5	0	3.47456	4.90651	0.01712	4.99757	4.17957
	Q_{c12}	0	5	0	3.78440	4.71029	0.14186	0.03554	4.07682
	Q_{c15}	0	5	0	2.76611	3.61236	0.02957	1.18163	4.17146
	Q_{17}	0	5	0	2.99716	0.01457	0.00000	0.72789	4.83945
	Q_{c20}	0	5	0	4.57258	4.58251	2.02777	4.97550	2.86524
	Q_{21}	0	5	0	4.98153	4.04716	0.00000	4.98735	3.04483
	Q_{c23}	0	5	0	2.50862	0.01196	0.00457	4.95938	4.94036
	Q_{24}	0	5	0	4.99707	4.28293	3.02812	4.96797	4.95660
	Q_{29}	0	5	0	2.10969	3.95118	0.63863	3.30036	4.99499
Tap Position	T_{11}	0.9	1.1	1.078	1.03080	1.04738	1.05597	1.01913	1.05077
	T_{12}	0.9	1.1	1.069	1.03860	1.03586	1.00876	1.04096	1.01569
	T_{15}	0.9	1.1	1.032	0.95241	0.99520	1.01355	0.95167	1.04096
	T_{36}	0.9	1.1	1.068	0.98279	1.00199	1.00406	0.97008	0.95084
GFC [USD/h]				901.639	**799.2557**	964.5746	936.1166	868.0514	834.0165
RPL [MW]				5.6891	8.6691	**2.9934**	3.5935	6.2099	6.3446
Em [ton/h]				0.2253	0.3681	0.2213	**0.2175**	0.2569	0.31
VD [p.u.]				1.1747	1.4192	1.4677	0.4754	**0.1097**	1.7545
VSI				0.1727	0.1237	0.1229	0.1483	0.1371	**0.1136**
Reduction rate				-	11.36%	47.38%	3.46%	90.66%	34.23%

The optimal values of the objective functions are given in bold.

- *Case #1:* To the optimal operating point, the generation fuel cost (GFC) used to operate generation units should be minimized by setting the control variables. Therefore, the first objective function of this study is to achieve generation fuel cost (GFC) minimization using the Slime Mould Algorithm (SMA). Table 3 illustrated that generation fuel cost has (GFC) been minimized to 799.2557 (USD/h). The remainder results of this case are 8.6691 (MW), 0.3681 (ton/h), 1.4192 (p.u.), and 0.1237 of RPL, Em, VD, and VSI.
- *Case #2:* The second objective function is to minimize the real power losses (RPL) in the transmission lines. The real power losses (RPL) will be reduced from 5.6891 (MW) at the initial case to 2.9934 (MW) at the optimal case with a reduction rate equal to 47.38%. The values of GFC, Em, VD, and VSI of this case are equal to 964.5746 (USD/h), 0.2213 (ton/h), 1.4677 (p.u.), and 0.1229, respectively.
- *Case #3:* Recently, emission (Em) studies have received growing attention due to environmental pollution and global warming. In this case, reducing emissions is the primary aim of the proposed SMA. The best result obtained by SMA to reduce emission is 0.2175 (ton/h). The reduction rate between the optimal case (0.2175(ton/h)) and the initial case (0.2253 (ton/h)) is 3.46%.
- *Case #4:* The fourth objective function in this paper is voltage deviation (VD) minimization. The aim of this minimizing is to improve voltage profiles at each load bus. The reduction rate of this case is 90.66% (compared between the initial case, which is 1.1747 (p.u.), and the optimal case, which is 0.1097 (p.u.)). The rest values of this case

are 868.0514 (USD/h), 6.2099 (MW), 0.2569 (ton/h), and 0.1371 of GFC, RPL, Em, and VSI, respectively.

- *Case #5:* To achieve more stability of whole power system, the voltage stability indicator (L_{max}) was minimized using the SMA. In this case, the VSI was minimized from 0.1727 at initial case to 0.1136 at the optimal case with a reduction rate equal to 34.23%. The remainder results of GFC, RPL, Em, and VD are 834.0165 (USD/h), 6.3446 (MW), 0.31 (ton/h), and 1.7545 (p.u.), respectively, as given in Table 3.

To demonstrate the effectiveness and superiority of SMA, the results of the objective function for five cases abstained by proposed approach SMA were compared with other meta-heuristics algorithm results reported in the literature. Tables 4 and 5 prove the effectiveness of performance SMA over the other recent algorithms. Figure 5a–e illustrates the convergence speed of single objective functions using the SMA optimization method to solve the OPF problem in the IEEE 30 bus test system. These figures prove the superiority and efficiency of the proposed approach by providing a good characteristics rate.

Table 4. Comparison of the results obtained by the SMA with other methods for Cases (1 and 2).

Case 1		Case 2	
Method	**GFC [USD/h]**	**Method**	**RPL (MW)**
Initial	901.6391	Initial	5.830
MSA [16]	800.5099	GWO [30]	3.51
SCA [36]	800.1018	SSA [30]	3.50
SSO [37]	802.2580	WOA [30]	3.50
DSA [38]	800.3887	MF [30]	3.50
JAYA [39]	800.479	HHO [30]	3.49
GPU-PSO [40]	800.53	SSO [37]	3.8239
SP-DE [41]	800.4131	EM [42]	3.1775
MGOA [43]	800.4744	EGA-DQLF [44]	3.2008
TLBO [45]	800.4604	ASO [46]	3.1600
AMTPG-Jaya [45]	800.1946	EGA-EA [47]	3.2601
GWO [48]	802.7924	GWO [48]	4.2905
ABC [49]	800.6850	PSO [50]	5.1957
IABC [49]	800.4215	HPSO-DE [50]	5.1476
EGA [51]	802.06	FAHSPSO-DE [50]	4.9989
IGA [52]	800.805	IPSO [53]	5.0732
AGAPOP [54]	799.8441	SMA	**2.9934**
ABC [55]	800.66		
PSOGSA [56]	800.49859		
GA [57]	800.5272		
IHS [57]	800.5202		
MFO [57]	800.7134		
ISSA [57]	800.4752		
SOS [58]	801.5733		
SMA	**799.2557**		

The values obtained by the proposed algorithm are given in bold.

Table 5. Comparison of the results obtained by the SMA with other methods for Cases (3, 4, and 5).

Case 3		Case 4		Case 5	
Method	**Em [ton/h]**	**Method**	**VD [p.u.]**	**Method**	**VSI**
Initial	0.3661	Initial	1.1747	Initial	0.1727
GWO [30]	0.2960	HFPSO [59]	0.1467	SSO [37]	0.1267
SSA [30]	0.2950	EJADE-SP [60]	0.3752	NISSO [37]	0.12547
WOA [30]	0.2950	MABC [61]	0.1292	Jaya [39]	0.1243
MF [30]	0.2950	SMA	**0.1097**	TLBO [45]	0.12444

Table 5. *Cont.*

Case 3		Case 4		Case 5	
Method	**Em [ton/h]**	**Method**	**VD [p.u.]**	**Method**	**VSI**
HHO [30]	0.2850			AMTPG-Jaya [45]	0.1240
SSO [37]	0.2315			ARCBBO [62]	0.1369
BSA [63]	0.2425			ECHT-DE [64]	0.13632
SMA	**0.2175**			SPEA [65]	0.1247
				DE [66]	0.1246
				SMA	**0.1136**

The values obtained by the proposed algorithm are given in bold.

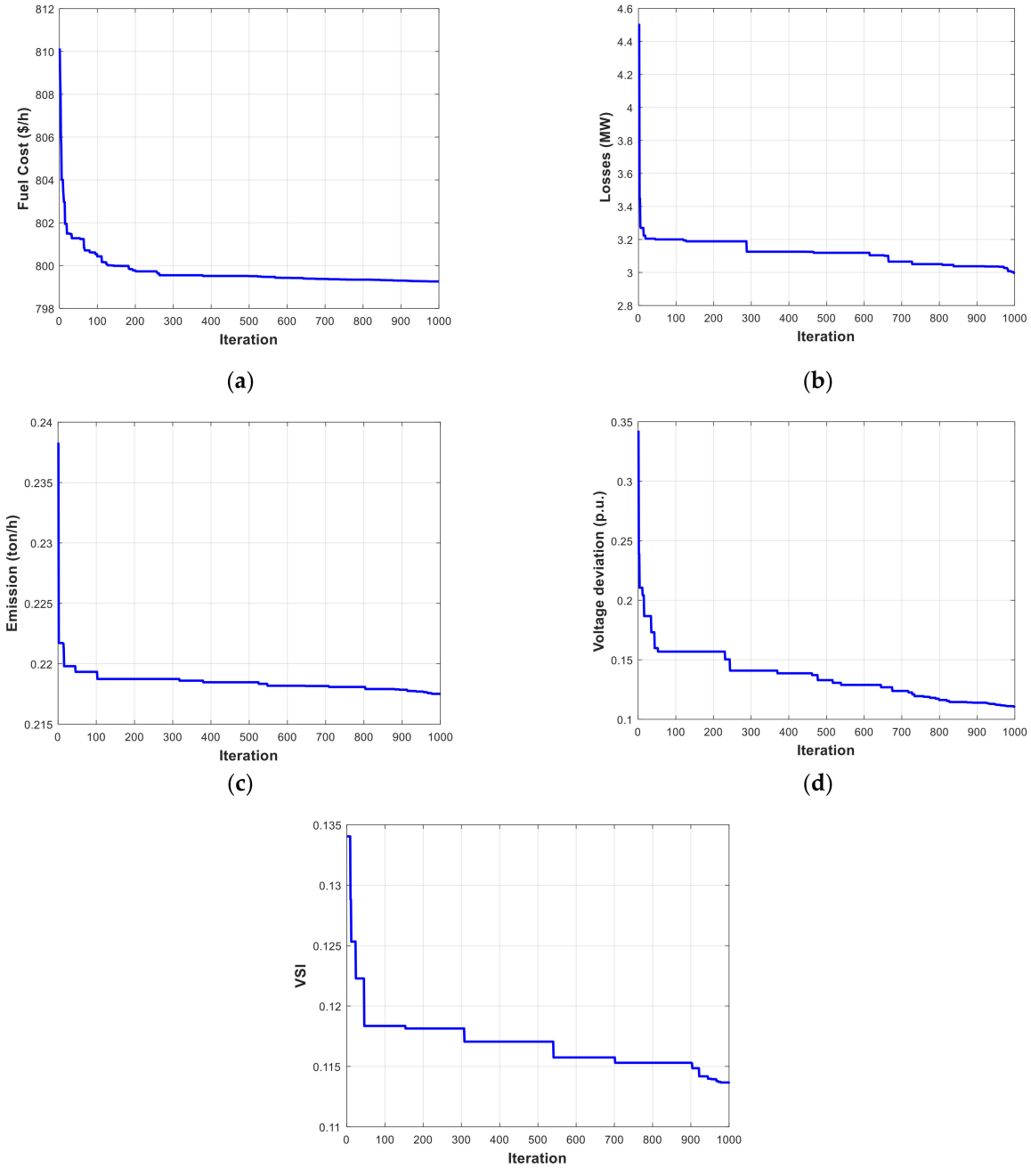

Figure 5. The convergence characteristics of the SMA algorithm for Cases 1–5. (**a**) Case 1, (**b**) Case 2, (**c**) Case 3, (**d**) Case 4, (**e**) Case 5.

5.1.2. Multiple-Objective OPF on IEEE 30-Bus Power System

To demonstrate the performance of the SMA on multi-objective optimization problems, MOSMA was applied to solve MOOPF problems. The number of populations is 500, and the stopping criteria of simulation running when no. of non-dominated solutions is equal to 500 or the no. of iterations equal to 500.

First, seven bi-objective functions (Cases 6–12) were studied and presented as follows:

- *Case #6:* In this case, MOSMA was applied to optimize the GFC and Em simultaneously. The best compromise solutions of GFC and Em are (832.8647 (USD/h), 0.2514 (ton/h)).
- *Case #7:* The GFC and RPL were optimized simultaneously. The best compromise solutions of GFC and RPL are (840.960 (USD/h), 4.8762 (MW)).
- *Case #8:* In Case 8, the two objectives function that were minimized and considered simultaneously are GFC and VD. The best compromise solution of this case is 802.0533 ($/h) and 0.3267 (p.u.) of GFC and VD, respectively.
- *Case #9:* The minimum GFC and VSI were simultaneously considered. The best compromise solutions obtained by MOSMA in this case are 800.1309 (USD/h) and 0.1172.
- *Case #10:* This case shows the minimization of Em and VD simultaneously. The proposed MOSMA provided the best compromise solutions, which are 0.2184 (ton/h) and 0.2074 (p.u.).
- *Case #11:* The RPL and VD were optimized simultaneously. The best compromise values obtained by the proposed MOSMA of RPL, and VD are 3.1922 (MW) and 0.5417 (p.u.), respectively.
- *Case #12:* The last case of the bi-objective functions type is the minimization of VD and VSI simultaneously. The proposed MOSMA provided the best compromise values for VD and VSI, which are 0.3102 (p.u.) and 0.1284, respectively.

The Pareto front, according to non-dominated solutions obtained by the proposed MOSMA of bi-objective functions, is shown in Figure 6a–g.

The Triple-objective functions are considered and presented as follows:

- *Case #13:* The GFC, RPL, and Em were presented as objective functions to optimize simultaneously. The best compromise of GFC, RPL, and Em obtained by the proposed MOSMA are 867.5282 (USD/h), 4.3416 (MW) and 0.2300 (ton/h), respectively.
- *Case #14:* In this case, the minimization of GFC, Em, and VD have been optimized simultaneously as objective functions. The best compromising GFC, Em, and VD obtained by the proposed approach are 841.554 (USD/h), 0.2531 (ton/h) and 0.2214 (p.u.), respectively.
- *Case #15*: In Case 15, the three objectives function that were minimized considered simultaneously are GFC, RPL, and VD. The best compromise values of this case are 844.6107 (USD/h), 6.0058 (MW), and 0.2279 (p.u.) of GFC, RPL, and VD, respectively.
- *Case #16:* The minimization of GFC, RPL, and VSI were optimized simultaneously. The best compromising of GFC, RPL, and VSI obtained by the proposed MOSMA are 841.4057 (USD/h), 5.0766 (MW) and 0.1176, respectively.
- *Case #17:* This case shows the minimization of GFC, Em, and VSI simultaneously. The proposed MOSMA provided the best compromise values, which are 850.7178 (USD/h), 0.2476 (ton/h), and 0.1158.
- *Case #18:* The GFC, VD, and VSI are optimized simultaneously. The best compromise values obtained by proposed MOSMA of GFC, VD, and VSI are 804.4035 (USD/h), 0.5409 (p.u.), and 0.1291 respectively.
- *Case #19:* The last case of triple-objective functions type is the minimization of Em, RPL, and VD simultaneously. The proposed MOSMA provided the best compromise values for Em, RPL, and VD are 0.2183 (ton/h), 3.9925 (MW) and 0.2414 (p.u.), respectively.

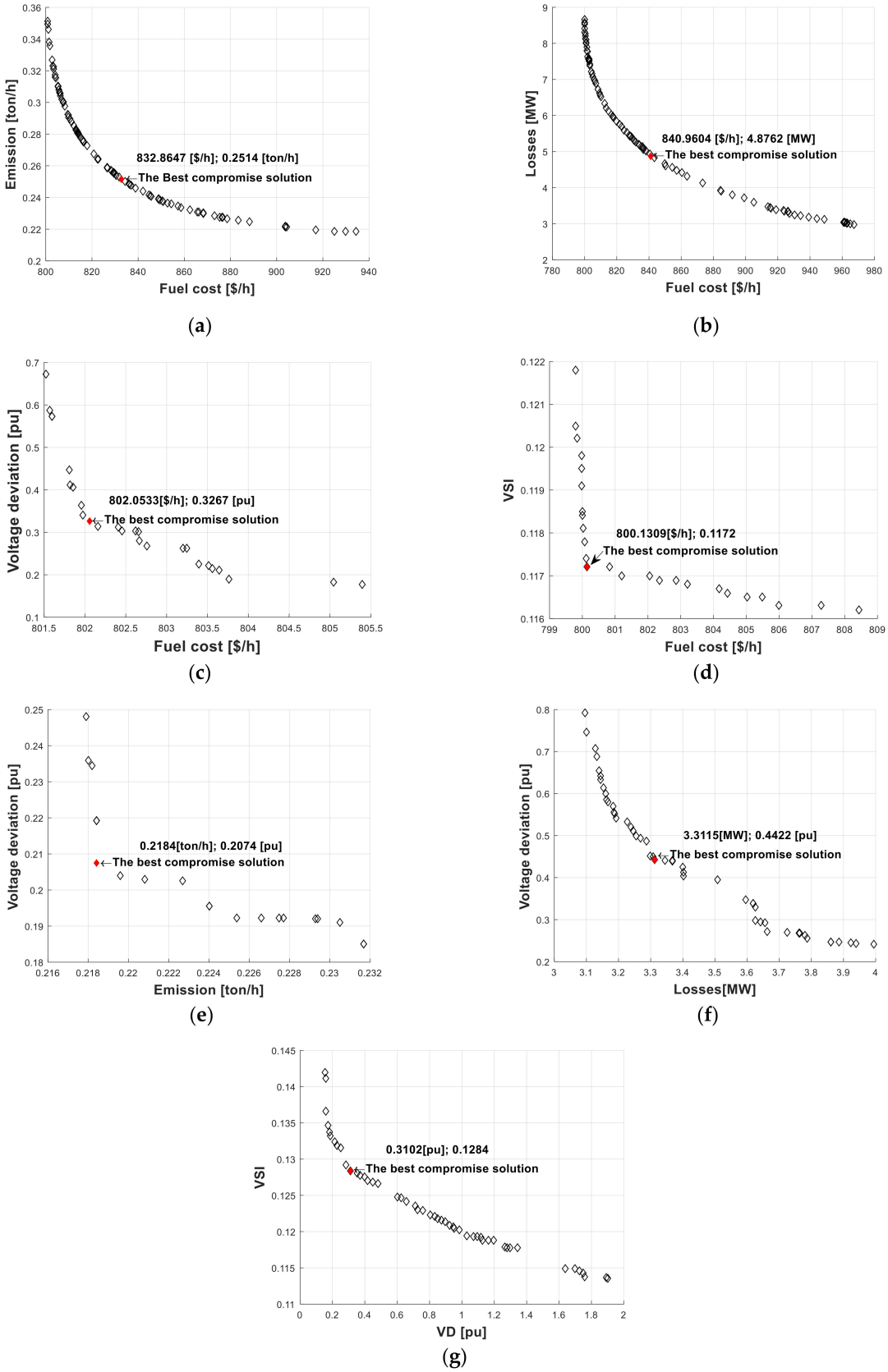

Figure 6. The convergence characteristics of the MOSMA algorithm for Cases 6–12. (**a**) Case 6, (**b**) Case 7, (**c**) Case 8, (**d**) Case 9, (**e**) Case 10, (**f**) Case 11, (**g**) Case 12.

The Pareto front, according to non-dominated solutions obtained by the proposed MOSMA of triple-objective functions, is shown in Figure 7a–g. The red diamonds indicate the best compromise solution of the triple objective functions for Cases 13–19.

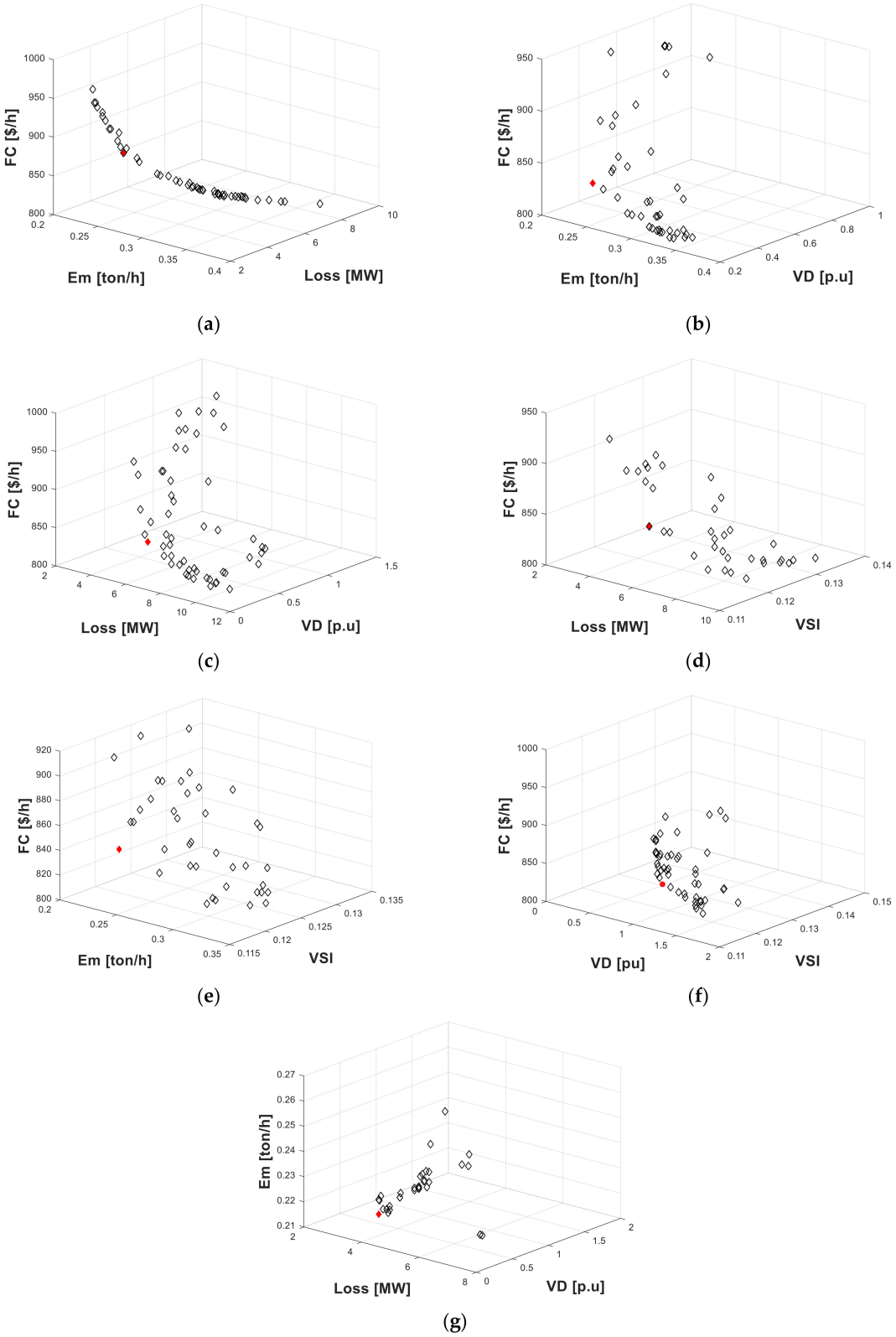

Figure 7. The convergence characteristics of the MOSMA algorithm for Cases 13–19. (**a**) Case 13, (**b**) Case 14, (**c**) Case 15, (**d**) Case 16, (**e**) Case 17, (**f**) Case 18, (**g**) Case 19.

Finally, the Quad and Quinta-objective functions are considered and presented as follows:

- *Case #20:* In this case, the GFC, Em, RPL, and VD were optimized simultaneously. The best compromise solutions obtained by the developed framework are 832.3665 (USD/h), 0.2675 (ton/h), 6.4495 (MW) and 0.2189 (p.u.), of GFC, Em, RPL, and VD, respectively.
- *Case #21:* The GFC, Em, RPL, and VSI were optimized simultaneously. The best compromising of GFC, Em, RPL, and VSI obtained by the proposed MOSMA are 847.723 (USD/h), 0.2466 (ton/h), 5.1423 (MW) and 0.1183, respectively.
- *Case #22:* The last case of the multiple-objective functions type is the minimization of GFC, Em, RPL, VD, and VSI simultaneously. The proposed MOSMA provided the best compromise values for GFC, Em, RPL, VD, and VSI, which are 824.7751 (USD/h), 0.2753 (ton/h), 6.3599 (MW), 0.5111 (p.u.) and 0.1290, respectively.

Tables 6 and 7 present the results of optimal control variables and objective functions obtained by the proposed MOSMA for Cases 6–22.

Table 6. Optimal control variables obtained by MOSMA for Cases 6–13.

Item		Case 6	Case 7	Case 8	Case 9	Case 10	Case 11	Case 12	Case 13
P_g [MW]	P_1	126.521	139.156	177.458	177.570	70.974	58.480	170.349	92.703
	P_2	57.394	48.924	46.455	50.162	70.791	77.896	70.719	68.717
	P_5	26.635	28.495	20.722	19.629	49.648	48.772	17.612	37.093
	P_8	34.242	34.955	21.449	18.869	34.749	33.597	19.081	34.532
	P_{11}	24.051	21.583	12.920	14.099	29.757	29.299	10.539	29.626
	P_{13}	20.555	16.447	14.204	12.017	32.509	39.018	14.182	25.070
V_g [p.u.]	V_1	1.098	1.100	1.045	1.099	0.988	1.042	0.958	1.097
	V_2	1.098	1.100	1.045	1.099	1.011	1.048	1.097	1.097
	V_5	1.098	1.100	1.045	1.099	1.079	1.017	0.959	1.097
	V_8	1.098	1.100	1.045	1.099	1.056	1.048	1.097	1.097
	V_{11}	1.098	1.100	1.045	1.099	1.098	1.095	1.035	1.097
	V_{13}	1.098	1.100	1.045	1.099	1.098	1.095	1.090	1.097
Shunt Element [MVAr]	Q_{c10}	0.001	1.014	0.279	0.047	0.001	0.001	0.486	1.097
	Q_{c12}	0.055	0.316	1.045	1.812	0.057	0.000	0.765	1.097
	Q_{c15}	0.000	0.326	0.440	0.116	0.004	0.005	0.179	0.124
	Q_{17}	0.485	0.469	0.015	0.229	0.000	0.000	1.097	0.976
	Q_{c20}	1.675	4.991	2.378	4.926	0.000	0.000	4.915	2.925
	Q_{21}	0.070	4.991	2.846	4.975	0.144	0.000	4.915	2.095
	Q_{c23}	0.325	4.991	2.916	4.972	0.000	0.007	4.915	3.283
	Q_{24}	0.003	4.991	1.608	4.972	0.001	1.029	4.915	2.774
	Q_{29}	0.043	2.394	0.775	4.972	1.335	0.000	4.915	0.822
Tap Position	T_{11}	1.023	0.999	1.007	1.005	1.014	1.022	1.063	1.027
	T_{12}	0.967	0.968	0.977	0.968	0.976	0.961	1.028	1.041
	T_{15}	1.006	0.989	0.962	1.022	0.965	1.006	0.971	0.952
	T_{36}	0.987	0.992	0.952	0.952	0.952	0.954	0.951	0.980
GFC [USD/h]		**832.8647**	**840.960**	**802.0533**	**800.1309**	935.1719	965.5084	866.5512	**867.5282**
RPL [MW]		5.4534	**4.8762**	9.6647	8.9461	5.0218	**3.1922**	15.0962	**4.3416**
Em [ton/h]		**0.2514**	0.2465	0.3826	0.3698	**0.2184**	0.2214	0.2713	**0.2300**
VD [p.u.]		0.9403	1.5133	**0.3267**	1.6453	**0.2074**	**0.5417**	**0.3102**	1.3322
VSI		0.1329	0.1243	0.1447	**0.1172**	0.1452	0.1370	**0.1284**	0.1288

The best compromise solutions for objective functions are given in bold.

Figure 8 shows the voltage profiles of all buses for Cases 1–22. Figure 8a shows the voltage profiles of all buses for Cases 1–5. Figure 8a proves that the proposed algorithm is effective only in Casess 3 and 4, but the results extracted from Cases 1, 2, and 5 are infeasible solutions because many load buses have voltage values exceeding the maximum limit for load buses, 1.05 (p.u.). Figure 8b shows the voltage profiles of the bi-objective function for Cases 6–12. Figure 8b proves that the proposed algorithm is effective only in cases in which the voltage deviation is considered an objective function, namely in Cases 8, 10, 11, and 12. However, the results obtained from cases that the voltage deviation is not considered an objective function for Cases 6, 7, and 9 are infeasible solutions because many load buses

have voltage values exceeding the maximum limit for load buses, 1.05 (p.u.). Figure 8c shows the voltage profiles of the triple-objective function for Cases 13–19. The proposed approach was effective for Cases 14, 15, 18, and 19. The cases that the voltage load bus exceeded the maximum limit for load buses, 1.05 (p.u.), are 13, 16, and 17. Figure 8d shows the voltage profiles of Quad and Quinta objective function for Cases 20–22. The results obtained by Case 21 are infeasible solutions because many load buses have voltage values exceeding the maximum limit for load buses, which is 1.05 (p.u.). The results obtained from cases (20,22) are effective because the value of the voltage load bus is within the range [0.95–1.05] (p.u.).

Table 7. Optimal control variables obtained by MOSMA for Cases (14–22).

Item		Case 14	Case 15	Case 16	Case 17	Case 18	Case 19	Case 20	Case 21	Case 22
P_g [MW]	P_1	113.137	118.406	117.802	103.918	170.859	71.869	129.158	111.560	135.012
	P_2	72.911	57.143	46.295	79.270	47.625	72.514	56.560	61.157	43.921
	P_5	28.035	36.667	34.245	21.055	25.984	49.962	36.327	34.110	29.727
	P_8	30.461	25.476	34.859	34.696	16.724	34.973	25.233	22.732	30.329
	P_{11}	24.979	22.381	29.887	29.757	17.284	29.979	22.187	29.610	24.467
	P_{13}	20.555	29.333	25.389	20.181	13.752	28.095	20.384	29.372	26.304
V_g [p.u.]	V_1	1.023	1.043	1.099	1.098	1.094	1.040	1.041	1.097	1.078
	V_2	0.985	1.043	1.099	1.098	1.094	1.027	1.041	1.097	1.073
	V_5	1.003	1.043	1.099	1.098	1.094	0.997	1.041	1.097	1.052
	V_8	1.074	1.043	1.099	1.098	1.094	1.009	1.041	1.097	1.064
	V_{11}	1.074	1.043	1.095	1.098	1.094	1.100	1.041	1.097	1.016
	V_{13}	1.061	1.043	1.099	1.098	0.968	1.036	1.041	1.097	1.039
Shunt Element [MVAr]	Q_{c10}	1.385	1.043	0.558	0.024	0.154	0.006	0.220	0.464	3.800
	Q_{c12}	0.294	1.043	1.034	0.316	0.127	0.043	1.041	0.965	1.808
	Q_{c15}	4.090	1.043	1.081	1.098	0.349	0.009	0.557	0.069	3.370
	Q_{17}	1.014	1.043	0.246	0.875	0.465	0.001	0.859	0.000	4.664
	Q_{c20}	1.994	3.095	4.972	4.939	1.710	3.970	1.570	0.877	3.839
	Q_{21}	0.010	3.095	4.227	4.939	0.083	0.792	2.404	4.903	4.180
	Q_{c23}	0.053	3.095	4.972	4.939	1.400	0.076	3.047	4.903	1.270
	Q_{24}	2.928	3.095	4.972	4.939	4.289	0.755	2.089	4.575	1.575
	Q_{29}	0.210	3.095	4.919	4.939	4.341	3.209	3.047	4.903	4.640
Tap Position	T_{11}	0.967	0.963	0.991	1.037	0.963	0.988	1.036	1.000	1.021
	T_{12}	1.049	0.985	1.029	0.990	1.097	0.971	0.979	0.957	0.990
	T_{15}	0.981	1.050	1.024	0.999	0.958	0.995	0.961	0.959	0.993
	T_{36}	0.953	0.953	0.963	0.951	0.952	0.961	0.965	0.954	0.956
GFC [USD/h]		**841.554**	**844.611**	**841.4057**	**850.7178**	**804.4035**	928.292	**832.3665**	**847.723**	**824.7751**
RPL [MW]		6.6773	**6.0058**	**5.0766**	5.4772	8.8206	**3.9925**	**6.4495**	**5.1423**	**6.3599**
Em [ton/h]		**0.2531**	0.2545	0.2502	**0.2476**	0.3495	**0.2183**	**0.2675**	**0.2466**	**0.2753**
VD [p.u.]		**0.2214**	**0.2279**	1.6214	1.7186	**0.5409**	**0.2414**	**0.2189**	1.6979	**0.5111**
VSI		0.1436	0.1370	**0.1176**	**0.1158**	**0.1291**	0.1440	0.1408	**0.1183**	**0.1290**

The best compromise solutions for objective functions are given in bold.

Figure 9 illustrates the reactive power output of generation units. From this figure, it can be observed that generator 1 exceeded the limits [−20 to 200 MVAr] in Cases 4, 5, 6, 10, 12, 16, and 17, while in the remaining cases, the constraints were not violated. The generators (2 and 8) violated the constraints in Case 12 only. The remaining generators (5, 11, and 13) satisfied all constraints in this study.

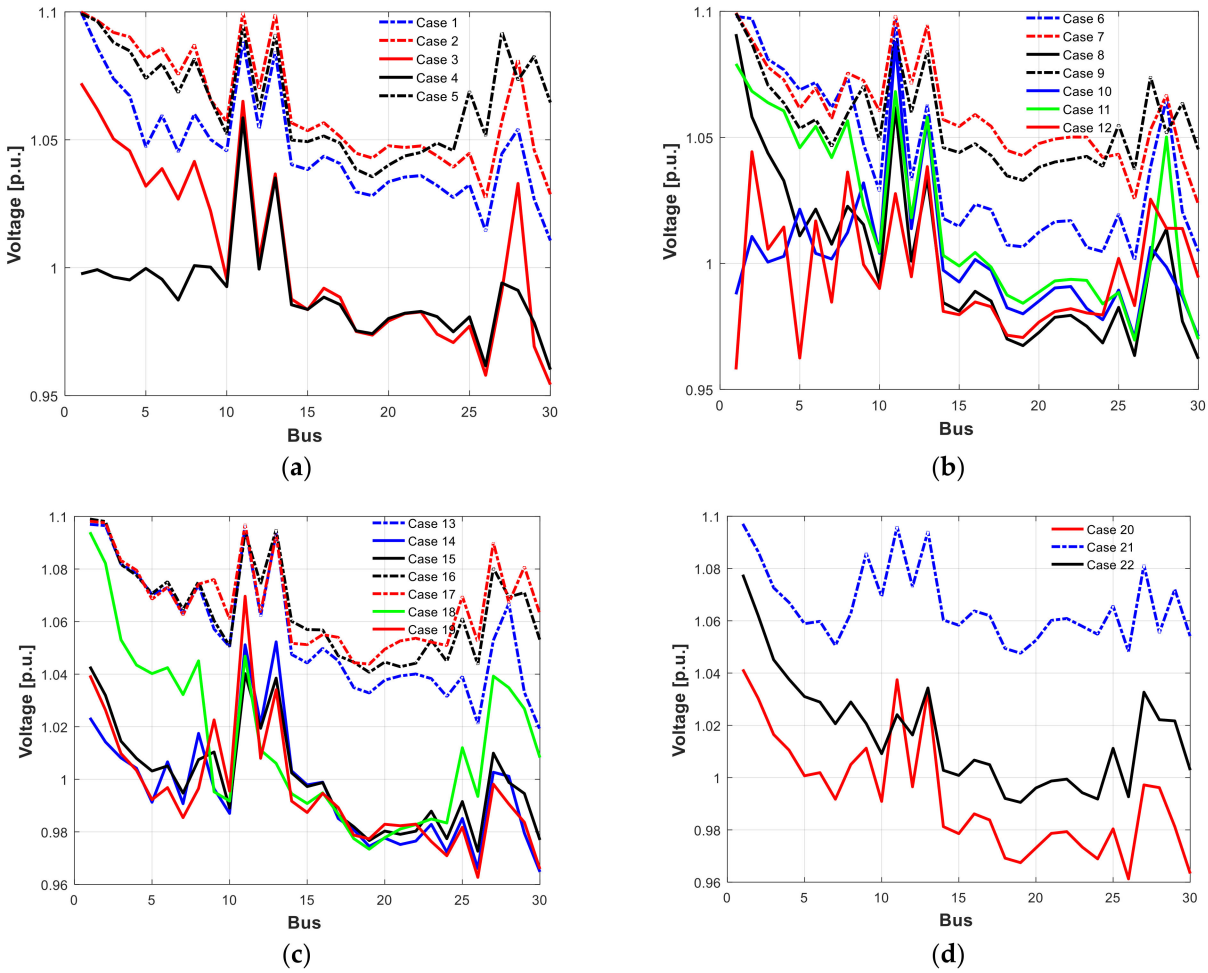

Figure 8. The voltage profile for single- and multi-objective optimal power flow on the IEEE 30-bus test system. (**a**) Single OF, (**b**) Bi OF, (**c**) Tri OF, (**d**) Quad and Quinta OF.

5.2. IEEE 57-Bus Power System

In this subsection, the IEEE 57- bus power system was applied to validate of performance of proposed MOSMA. The total generation capacity of this system is 1975.9 MW [34]. The main characteristics of IEEE 57- bus power system is given in Table 1. Figure A2 represents the single-line diagram of the IEEE 57 bus system. The coefficients of the cost and emission of generators are given in Table A2.

Single-Objective OPF on IEEE 57-Bus Power System

To demonstrate the superiority and performance of the proposed method on IEEE 57- bus power system, three single objective functions (Cases 23–25) were considered. The number of iterations and population sizes are 1000 and 250, respectively. Table 8 represents the optimal setting of control variables and optimal results of objective functions obtained by proposed method. The convergence speed of proposed method is illustrated in Figure 10a–c.

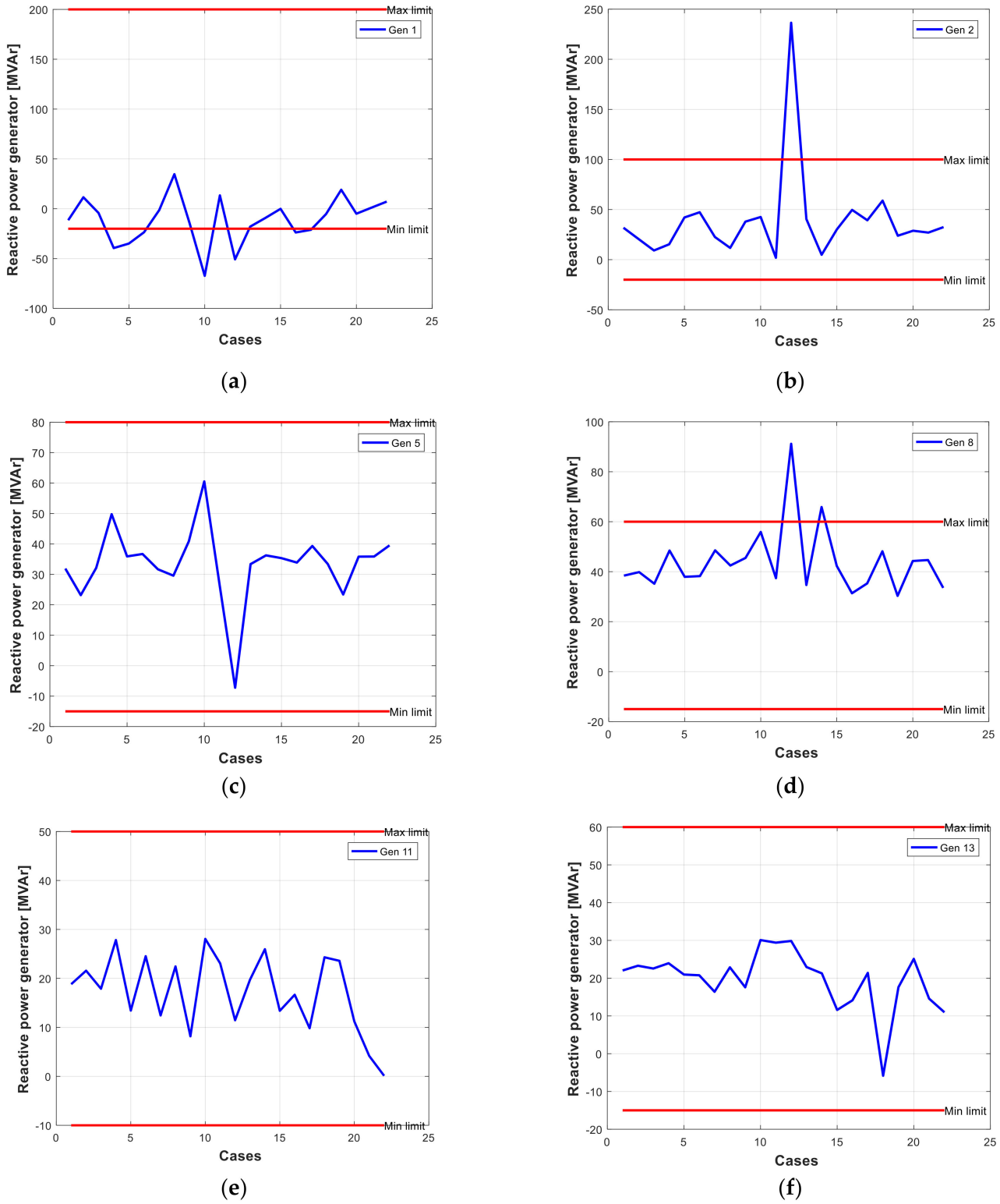

Figure 9. The reactive power output of generators for Cases 1-22 on the IEEE 30-bus system. (**a**) Generator 1, (**b**) Generator 2, (**c**) Generator 5, (**d**) Generator 8, (**e**) Generator 11, (**f**) Generator 13.

Table 8. Optimal control variables obtained by the SMA algorithm for Cases 23-25 on the IEEE 57-bus system.

	Item	Max	Min	Initial	Case 23	Case 24	Case 25
[MW]	P_1	0.0	576	478	142.26	188.27	188.26
	P_2	30.0	100	0	89.97	99.58	22.33
	P_3	40.0	140	40	45.18	139.66	139.83
	P_6	30.0	100	0	70.04	99.56	99.80
	P_8	100.0	550	450	463.46	276.00	300.14
	P_9	30.0	100	0	94.12	99.95	99.78
	P_{12}	100.0	410	310	359.91	362.06	409.74
[p.u.]	V_1	0.95	1.10	1.040	1.08	1.07	1.10
	V_2	0.95	1.10	1.010	1.08	1.08	1.10
	V_3	0.95	1.10	0.985	1.08	1.06	1.10
	V_6	0.95	1.10	0.980	1.09	1.05	1.10
	V_8	0.95	1.10	1.005	1.10	1.07	1.10
	V_9	0.95	1.10	0.980	1.09	1.08	1.09
	V_{12}	0.95	1.10	1.015	1.08	1.07	1.09
Tap Position	T_{4-18}	0.90	1.10	0.97	0.97	0.99	1.07
	T_{4-18}	0.90	1.10	0.978	1.00	1.02	0.98
	T_{21-20}	0.90	1.10	1.043	0.95	1.06	1.04
	T_{24-25}	0.90	1.10	1	0.97	1.04	1.01
	T_{24-25}	0.90	1.10	1	0.95	1.04	0.97
	T_{24-26}	0.90	1.10	1.043	0.97	1.05	1.02
	T_{7-29}	0.90	1.10	0.967	0.98	1.03	0.98
	T_{34-32}	0.90	1.10	0.975	0.98	0.97	1.01
	T_{11-41}	0.90	1.10	0.955	0.99	1.08	1.00
	T_{15-45}	0.90	1.10	0.955	1.00	1.05	0.96
	T_{14-46}	0.90	1.10	0.9	1.00	1.07	0.96
	T_{10-51}	0.90	1.10	0.93	1.01	1.03	0.97
	T_{13-46}	0.90	1.10	0.895	0.97	1.00	0.95
	T_{11-43}	0.90	1.10	0.958	0.96	1.04	0.98
	T_{40-56}	0.90	1.10	0.958	0.97	0.98	1.02
	T_{39-57}	0.90	1.10	0.98	0.96	1.03	1.04
	T_{9-55}	0.90	1.10	0.94	0.99	1.06	0.98
[MVAr]	Q_{c18}	0.00	20.0	10	12.11	0.00	20.00
	Q_{25}	0.00	20.0	5.9	5.04	11.87	14.57
	Q_{53}	0.00	20.0	6.3	15.29	19.68	12.81
FC [USD/h]				51353	**41633.61**	45157	44911
Em [ton/h]				2.4129	1.3624	**0.9595**	1.1126
RPL [MW]				27.868	14.3018	14.7671	**9.2874**
VD [p.u.]				1.1264	2.4684	2.5298	3.8873
VSI					0.2561	0.2890	0.2145
Reduction rate				-	18.93%	60.24%	66.67%

The optimal values of objective function are given in bold.

- *Case #23:* The GFC is the objective function that has been considered. The minimum of GFC obtained by the proposed method is 41633.61 (USD/h). The remainder results of this case are 14.3018 (MW), 1.3624 (ton/h), 2.4684 (p.u.), and 0.2561 of RPL, Em, VD, and VSI, respectively. The reduction rate between the optimal case and the initial case is 18.93%.
- *Case #24:* The minimization of Em is the objective function of this case. The optimal result obtained from this case is 0.9595 (ton/h) using the proposed approach. The reduction rate of emission reaches 60.24% when compared to the initial case (2.4129 (ton/h)) and the optimal case (0.9595 (ton/h)). The rest values of GFC, RPL, VD, and VSI are 45157 (USD/h), 14.7671 (MW), 2.5298 (p.u.), and 0.2890, respectively.
- *Case #25:* The main objective function of this case is the reduction of RPL. The best result obtained by the proposed approach is 9.2874 (MW) with a reduction rate equal to 66.67%. The remainder values of GFC, Em, VD, and VSI are 44911 (USD/h), 1.1126 (ton/h), 3.8873 (p.u.), and 0.2145, respectively.

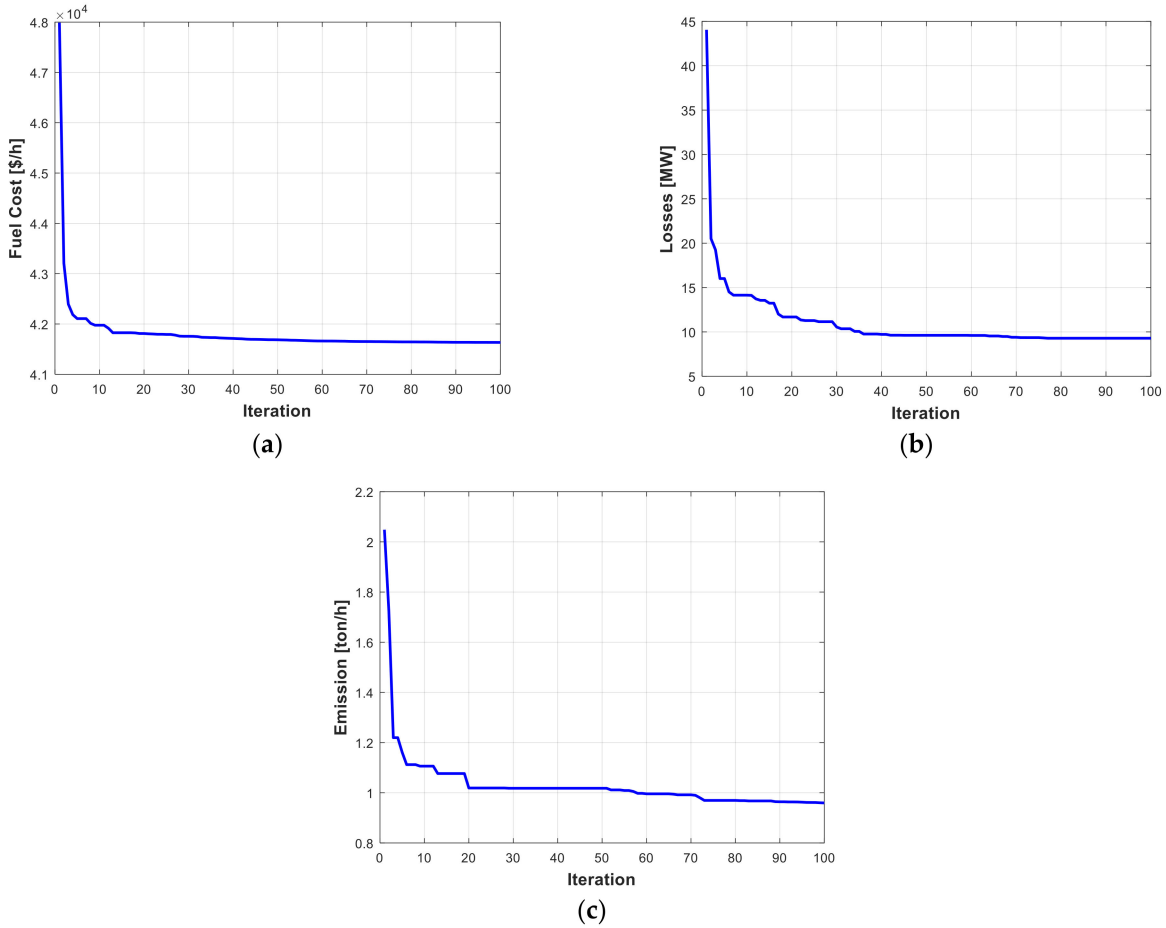

Figure 10. The convergence characteristics of the SMA for Cases 23–25. (**a**) Case 23, (**b**) Case 24, (**c**) Case 25.

To prove the superiority and performance of the SMA on the IEEE 57-bus system, the optimal results of the objective function obtained by the proposed approach SMA were compared with the optimal results obtained by other recent optimization methods reported in the literature. Table 9 proved the effectiveness of proposed algorithm over the other recent algorithms. Figure 9a–c shows the convergence rate of single-objective functions using the SMA optimization method to solve the OPF problem in the IEEE 57-bus test system. These figures prove the superiority and efficiency of the proposed approach by providing a good characteristics rate.

5.3. Iraqi Super Grid High Voltage 400 kV (ISGHV 400 kV)

The Iraqi Super Grid High Voltage 400 kV (ISGHV 400 kV) has been chosen as practical system to prove the ability and applicability of the proposed SMA as shown in Figure A3 [67]. The main characteristics of ISGHV is given in Table 1. The bus number 01 (MUSP) represents the swing bus, and the total load demand is 5994 MW. Table A3 presents the cost coefficients of the ISGHV network. The nodes and lines data of the ISGHV (400 kV) [68] are detailed in Tables A4 and A5 respectively.

Single-Objective OPF on ISGHV 400 kV

- *Case #26:* The objective function in this case is the minimization of GFC of the ISGHV network. The GFC was reduced from 39565 (USD/h) in the initial case to 20740 (USD/h) in the optimal case, with a reduction rate equal to 47.58%. The GFC, VD, and VSI are equal to 45.2254 (MW,) 0.4678 (p.u.) and 0.0826, respectively, as tabulated in Table 10.

- *Case #27:* In this case, the objective function that was optimized is RPL by means of SMA. The optimal result of RPL was reduced to 18.6087 (MW) compared with the initial case, which was equal to 42.3834 (MW) The reduction rate of this case is 56.09%. The rest results of GFC, VD, and VSI are equal to 36784 (USD/h), 0.7725 (p.u.) and 0.0815, respectively, as tabulated in Table 10.
- *Case #28:* The third objective function of this subsection is to improve the voltage profiles by minimizing the voltage deviation (VD) at the load bus from 1.0 (p.u.) The VD was minimized from 0.2013 (p.u.) in the initial case to 0.0625 (p.u.) in the optimal case. The reduction rate of VD is 68.95%.

The remainder results of GFC, RPL, and VSI are equal to 49843 (USD/h), 54.8430 (MW), and 0.0917, respectively, as tabulated in Table 10.

- *Case #29:* The last case of this article is the voltage stabilization reinforcement by minimization of the maximum voltage stability index (L-index) of the system load buses. The VSI is minimized to 0.0749 in the optimal case compared with 0.0886 in the initial case. The reduction rate of VSI is 15.46%. The GFC, RPL, and VD are equal to 45500 (USD/h), 19.9760 (MW), and 1.2955 (p.u.), respectively, as tabulated in Table 10.

Figure 11a–d illustrates the convergence rate single-objective functions using the SMA optimization method to solve the OPF problem in the ISGHV 400 kV network. The optimal control variables obtained by the proposed method provide the optimal objective functions tabulated in Table 10.

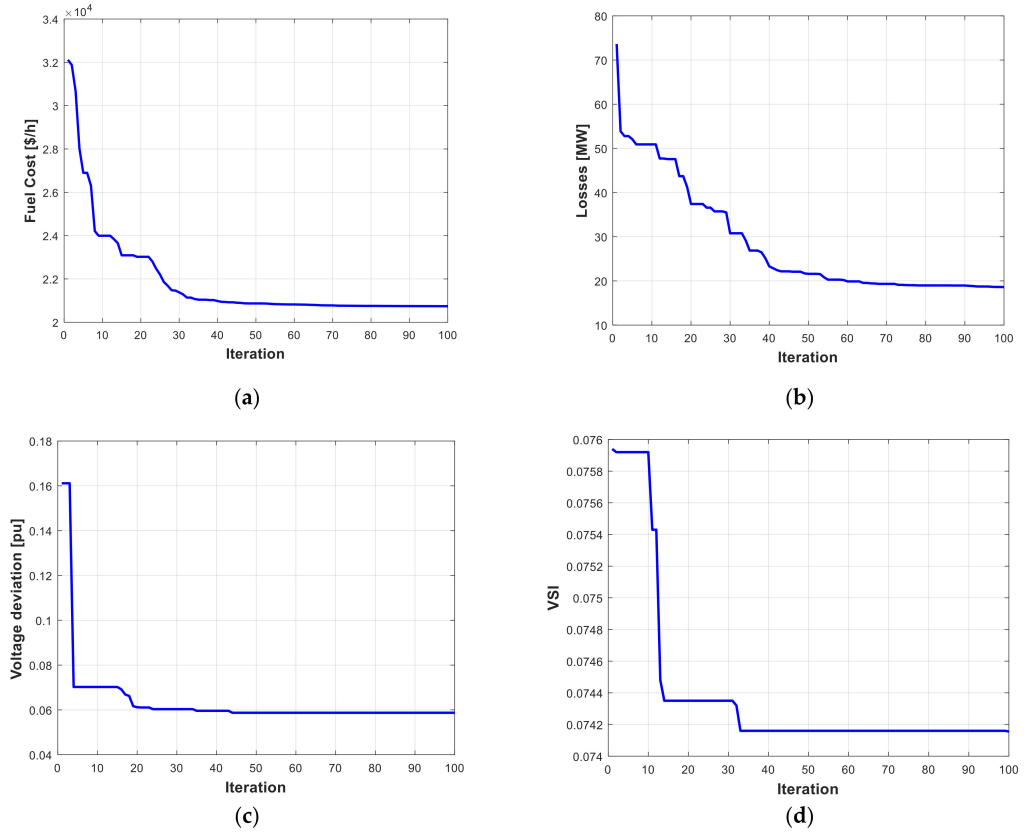

Figure 11. The convergence characteristics of the SMA algorithm for Cases 26–29 on the ISGHV 400 kV network. (**a**) Case 26, (**b**) Case 27, (**c**) Case 28, (**d**) Case 29.

5.4. Performance Comparison

This subsection presents the performance and efficiency of the proposed approach (SMA and MOSMA) to solve single- and multi-objective optimal power flow problems. The standards and all their variants were evaluated to solve real-world problems. The SMA and MOSMA were carried out on all cases to achieve the best solutions for single- and

multi-objective problems. The researchers faced two main challenges to solve single- and multi-OPF problems: the speed convergence toward the global optimum (single and multi OF) and the good distribution of the Pareto front (Multi OF). In other words, the balance between convergence and coverage should be found to determine the effectiveness of the algorithm. For example, the results obtained by the proposed algorithm from Cases 1–5 were compared with other recent algorithms as shown in Tables 4, 5 and 9. These results confirmed the efficiency and superiority of the proposed algorithm. It is worth mentioning that none of the meta-heuristics algorithms can be superior to all optimization algorithms in solving all optimization problems, according to the no free lunch theorem (NFL) [69]. This is the main reason leading to no superior algorithm on all sides (coverage and convergence). This is very clear when applying the proposed approach to multi-objective functions. Therefore, it is difficult to compare the proposed approach MOSMA with other methods in terms of the results.

Table 9. Comparison of the results obtained by SMA with other methods from Cases 23-25 on the IEEE 57-bus system.

Case 23		Case 24		Case 25	
Method	**FC [USD/h]**	**Method**	**Em [ton/h]**	**Method**	**RPL [MW]**
Initial	51353	Initial	2.4129	Initial	27.8683
TLBO [43]	41683	PSO [27]	1.19	PSO [27]	13.6673
GA [43]	41685	GA [27]	1.189	GA [27]	13.3983
GOA [43]	41680	Jaya [27]	1.1111	ABC [49]	12.6260
ABC [55]	41694	SSO [37]	1.7024	MICA [70]	11.8826
MO-DEA [71]	41683	NISSO [37]	1.03927	SMA	**9.2874**
GSA [72]	41695	ABC [49]	1.2048		
NPSO [73]	41699.52	IABC [49]	1.0484		
KHA [74]	41709.3	MICA [70]	1.2246		
EADDE [75]	41713.6	MTLBO [76]	1.0772		
fuzzy GA [77]	41716.3	GBBICA [78]	1.1724		
SMA	**41633.61**	SKHA [79]	1.08		
		SMA	**0.9595**		

The optimal values of objective function are given in bold.

Based on the above, the simulation results obtained by the SMA and MOSMA for both single- and multi-objective functions have a high performance and provide high-quality solutions to solve OPF problems. The computational times of proposed approach (SMA and MOSMA) are competitive compared to other recent algorithms. In the multi-objective function and based on high-quality random search property of MOSMA, the objective functions (despite conflict with each other) provide the trade-off solutions among of each objective function. In Pareto fronts, the MOSMA provides good convergence, high efficiency, and a good distribution of two and three dimensions.

Table 10. Optimal control variables obtained by the SMA for four cases on the ISGHV network.

	Item	**Max**	**Min**	**Initial**	**Case 26**	**Case 27**	**Case 28**	**Case 29**
[MW]	P_1	150	1200	159.383	1096.691	813.1153	1158.4575	888.0881
	P_2	130	988	690	987.9720	325.8517	447.2378	351.6373
	P_3	250	750	250	250.0141	384.4645	434.8705	284.2415
	P_4	120	1320	406	120.0362	395.7200	563.6893	305.5577
	P_5	120	636	591	120.0380	170.0734	310.7864	614.2338
	P_6	50	260	240	50.2201	73.2614	127.6456	65.0107
	P_7	180	910	735	732.5920	896.2568	449.9110	879.2067
	P_8	60	660	203	659.9335	427.6555	281.8446	166.4127
	P_9	50	500	369	67.3979	152.3144	216.3835	155.9652

Table 10. *Cont.*

Item		Max	Min	Initial	Case 26	Case 27	Case 28	Case 29
[p.u.]	P_{10}	250	1320	478	250.0869	559.2488	645.6229	416.5426
	P_{11}	250	1250	600	583.3062	288.9408	619.7411	406.4446
	P_{12}	210	840	775	635.0647	837.6637	442.9369	813.4249
	P_{13}	100	440	332	435.5222	439.0323	225.7120	425.6579
	P_{14}	50	250	208	50.3508	248.9596	123.9482	241.5635
	V_1	0.95	1.1	1.04	1.0394	1.0592	1.0055	1.0937
	V_2	0.95	1.1	1.02	1.0305	1.0609	1.0055	1.0937
	V_3	0.95	1.1	1.01	1.0089	1.0586	1.0055	1.0937
	V_4	0.95	1.1	1.02	1.0182	1.0604	1.0055	1.0937
	V_5	0.95	1.1	1.02	1.0180	1.0604	1.0055	1.0937
	V_6	0.95	1.1	1.02	1.0281	1.0562	1.0055	1.0937
	V_7	0.95	1.1	1.01	1.0305	1.0567	1.0055	1.0937
	V_8	0.95	1.1	1.02	1.0286	1.0614	1.0055	1.0937
	V_9	0.95	1.1	1.02	1.0398	1.0582	1.0055	1.0937
	V_{10}	0.95	1.1	1.03	1.0507	1.0652	1.0055	1.0937
	V_{11}	0.95	1.1	1.03	1.0530	1.0594	1.0055	1.0937
	V_{12}	0.95	1.1	1.02	1.0647	1.0682	1.0055	1.0937
	V_{13}	0.95	1.1	1.01	1.0448	1.0459	1.0055	1.0937
	V_{14}	0.95	1.1	1.01	1.0448	1.0497	1.0055	1.0937
FC [USD/h]				39565	**20740**	36784	49843	45500
RPL [MW]				42.3834	45.2254	**18.6087**	54.8430	19.9760
VD [p.u.]				0.2013	0.4678	0.7725	**0.0625**	1.2955
VSI				0.0886	0.0826	0.0815	0.0917	**0.0749**
Reduction rate				-	47.58%	56.09%	68.95%	15.46%

The optimal values of the objective function are given in bold.

6. Conclusions

In this paper, a new meta-heuristic optimization algorithm inspired by the diffusion and foraging conduct of slime mould, called the Slime Mould Algorithm, was proposed to solve single- and multi-objective OPF problems. The objective functions that were considered are the generation fuel cost (GFC), real power losses (RPL) in the transmission lines, total emission (Em) issued by fossil-fuelled generation units, voltage deviation (VD) at buses, and voltage stability index (VSI) of whole system. The Pareto concept is the approach proposed to solve multi-objective OPF problems by determining the set of non-dominated solutions (Pareto front). The theory used to extract the best compromise solution is fuzzy set theory. In multiple-objective functions, MOSMA was developed to find optimal solution for two to five conflicting objective functions simultaneously. To validate the MOSMA performance, three different power systems were applied, two standard IEEE test systems (IEEE 30-bus and IEEE 57- bus power systems) and one practical system (Iraqi Super Grid High Voltage 400 kV), with 29 case studies of single- and multi-objectives functions. The simulations results confirmed that the convergence speed of SMA is impressive. To demonstrate the robustness and superiority of SMA, the optimal results of objective function was compared with other recent meta-heuristics optimization methods. The SMA provides a favourable performance, competitive optimizer, and better convergence speed to solve OPF problems in the power system.

Author Contributions: Conceptualization, M.A.-K. and V.D.; methodology, M.A.-K.; software, M.A.-K.; validation, M.A.-K., V.D. and M.E.; formal analysis, M.A.-K.; investigation, M.A.-K. and V.D.; data curation, M.A.-K.; writing—original draft preparation, M.A.-K.; writing—review and editing, V.D. and M.E.; visualization, M.A.-K. and V.D.; supervision, V.D. and M.E.; project administration, M.E.; funding acquisition, V.D. All authors have read and agreed to the published version of the manuscript.

Funding: This research received no external funding.

Data Availability Statement: Not applicable.

Conflicts of Interest: The authors declare no conflict of interest.

Abbreviations

OPF	Optimal power flow
OF	Objective function
SMA	Slime Mould Algorithm
MOSMA	Multi-Objective Slime Mould Algorithm
MOSMA	Multi-Objective Slime Mould Algorithm
GFC	Generation fuel costs
RPL	Real power losses
Em	Emission
VD	Voltage deviation
VSI	Voltage stability index
ISGHV	Iraqi Super Grid High Voltage
NFL	No free lunch theorem
Nomenclature	
f, g_i, and h_i	Objective functions, equality, and inequality constraints, respectively
u and x	The control and state variables, respectively
n, m, and p	Number objectives functions, number of equality constraint, and number of inequality constraint, respectively
P_G and Q_G	The real and reactive power output of generation units, respectively
V_G and V_L	The voltages magnitude at PV and PQ buses, respectively
T	The tap setting ratio of transformers
Q_c	The source VAR compensators
N_G,N_T,N_C,N_L, N_B, and N_{nl}	The numbers of generators, regulating transformers, shunt compensators units, load buses, all buses, and transmission lines, respectively
a_i, b_i and c_i	Generation fuel cost coefficients of generators
G_{ij} and B_{ij}	The conductance and susceptance, respectively
S_{L_m}	The apparent power flow in each transmission line
α_i,β_i,γ_i,ζ_i,and λ_i	The emission coefficients of generators
Y_L and Y_G	The submatrix of the original admittance Y_{bus}, respectively
t	The current iteration
δ	The angle difference between phase i and phase j
ub	The parameter in the range $[-a, a]$
uc	decreases linearly [1−0]
Y_b	The population position according to the highest concentration of odour currently found
Y	The slime mould location
Y_A and Y_B	The individuals have been chosen as randomly of slime mould, respectively
W	The weight of slime mould
fit, and df	The fitness and best fitness value of Y, respectively
t_max	The maximum iteration
$R(i)$	The ranks first half of the population
$rand$ and r	denotes the random value within $[0, 1]$
bf, and wf	denotes the optimal and worst fitness, respectively
$SmIndex$	refers to the sequence of fitness values sorted
lb and ub	indicate to the limit of lower and upper boundaries
z	The value of the parameter-setting experiment that will be discussed
F_i^{min} and F_i^{max}	Minimum and maximum value of objective function
u^k	The membership function
M	The total number of non-dominated solutions
u_i^k	The weight factor of the $i-th$ objective function

Appendix A

Table A1. The coefficients of cost and emission of generators for the IEEE 30-bus test system.

	Coefficient Generating Unit					
	G1	G2	G5	G8	G11	G13
	Fuel cost coefficient					
a	0	0	00	0	0	0
b	2	1.75	1	3.25	3	3
c	0.00375	0.0175	0.0625	0.00834	0.025	0.025
	Emission coefficient					
α	4.091	2.543	4.258	5.326	4.258	6.131
β	−5.554	−6.047	−5.094	−3.55	−5.094	−5.555
γ	6.49	5.638	4.586	3.38	4.586	5.151
ζ	2.00×10^{-4}	5.00×10^{-4}	1.00×10^{-6}	2.00×10^{-3}	1.00×10^{-6}	1.00×10^{-5}
λ	2.857	3.33	8	2	8	6.67

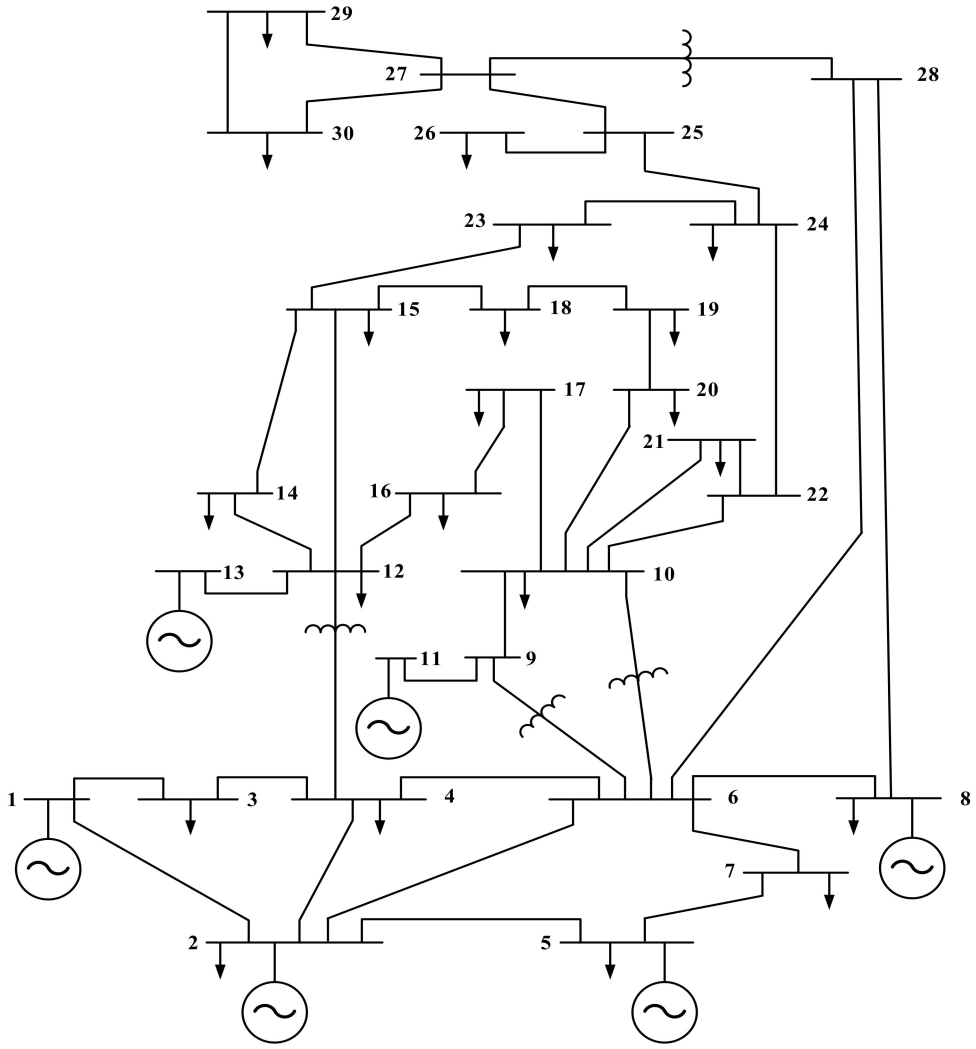

Figure A1. Single-line diagram of the IEEE 30-bus system.

Table A2. The coefficients of cost and emission of generators for the IEEE 57-bus test system.

	Coefficient Generating Unit						
	G1	G2	G3	G6	G8	G9	G12
	Fuel cost coefficient						
a	0	0	0	0	0	0	0
b	2	1.75	3	2	1	1.75	3.25
c	0.00375	0.0175	0.025	0.00375	0.0625	0.0195	0.00834
	Emission coefficient						
α	4.091	2.543	6.131	3.491	4.258	2.754	5.326
β	−5.554	−6.047	−5.555	−5.754	−5.094	−5.847	−3.555
γ	6.49	5.638	5.151	6.39	4.586	5.238	3.38
ζ	2.0×10^{-4}	5.0×10^{-4}	1.0×10^{-5}	3.0×10^{-4}	1.0^{-6}	4.0×10^{-4}	2.0×10^{-3}
λ	2.857×10^{-1}	3.33×10^{-1}	6.67×10^{-1}	2.66×10^{-1}	8.0×10^{-1}	2.88×10^{-1}	2.0×10^{-1}

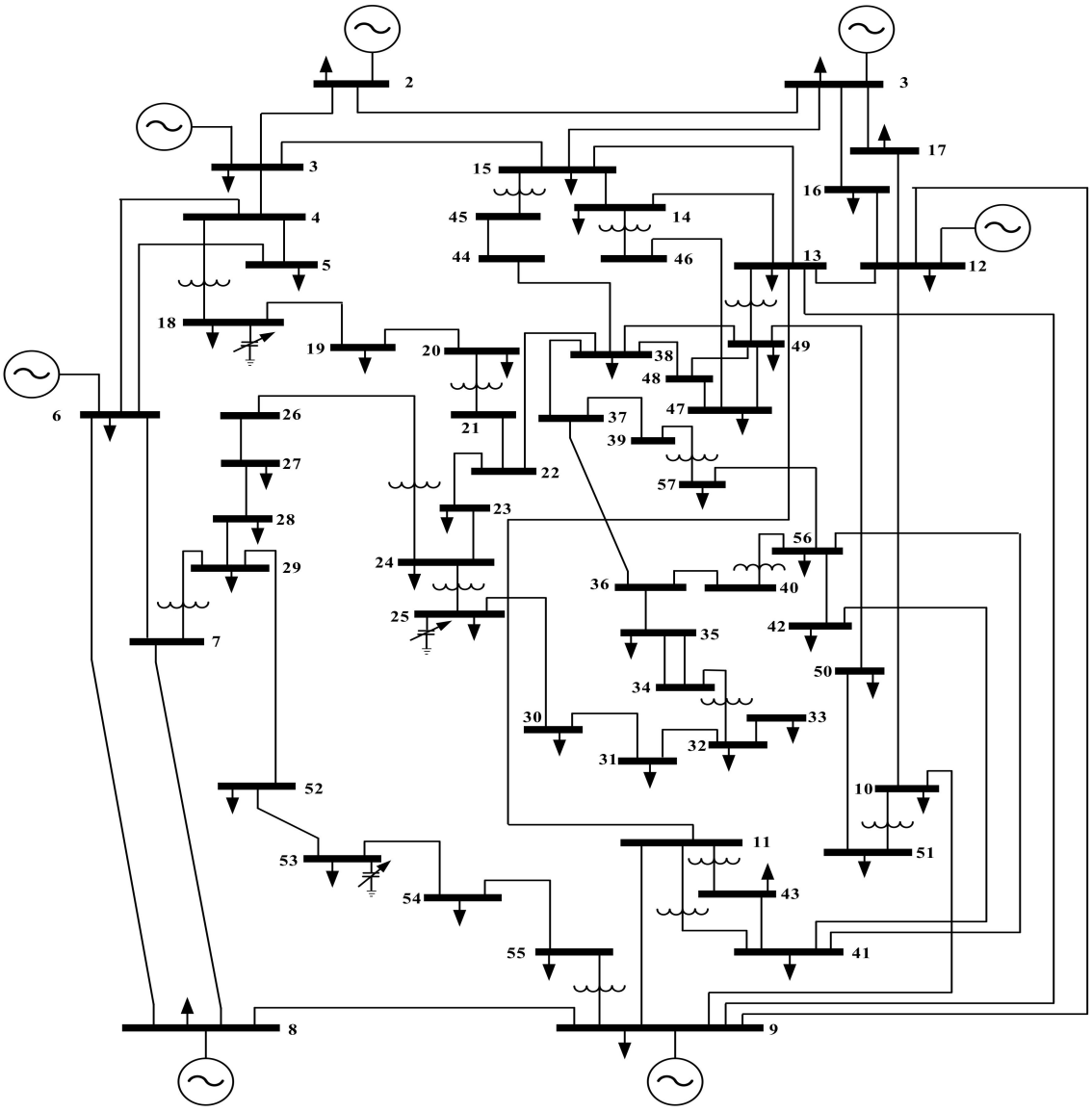

Figure A2. Single-line diagram of the IEEE 57-bus system.

Table A3. The cost coefficients of generators for the ISGHV network.

Gen	*a*	*b*	*c*	Gen	*a*	*b*	*c*
1	275	0.35	0.0012	8	0	0	0
2	0	0	0	9	250	0.5	0.02
3	200	3.5	0.04	10	300	2.2	0.003
4	2581	2.155	0.05	11	200	0.652	0.002
5	1698	11.91	0.03	12	159	0.561	0.002
6	154	7.05	0.0136	13	120	0.8	0.0025
7	200	0.64	0.0017	14	685	3.1	0.0158

Table A4. The node's data of ISGHV (400 kV).

Bus No.	Type	Bus Name	Voltage		Load		Generation		Q Injection
			Mag [p.u.]	Angle Deg.	MW	MVAr	MW	MVAr	
1	Slack	MUSP	1.04	0	206	56	159.4	2347.4	0
2	PU	MMDH	1.015	9.525	0	0	690	−92.4	0
3	PU	GNENW	1.01	7.695	150	75	250	−120.3	0
4	PU	BAJP	1.02	6.74	125	93	406	−203.8	−155
5	PU	BAJG	1.02	6.792	0	0	591	−91	0
6	PU	KRK4	1.017	5.691	130	10	240	−194	−100
7	PU	QDSG	1.01	−0.773	0	0	735	115.6	0
8	PU	HDTH	1.02	2.645	200	50	203	−198.7	0
9	PU	MUSG	1.02	0.243	0	0	369	−2082.4	0
10	PU	KUTP	1.03	−0.654	0	0	478	−70	0
11	PU	GKHRP	1.025	1.618	0	0	600	−295.4	0
12	PU	NSRP	1.02	−2.117	423	101	775	−230.3	−100
13	PU	HRTHP	1.01	−9.663	155	72	332	69.9	−50
14	PU	KAZG	1.0096	−9.48	200	101	208	24.6	−50
15	PQ	MSL4	1.0119	7.252	650	302	0	0	−50
16	PQ	BGS4	1.0246	−0.671	0	0	0	0	0
17	PQ	BGW4	1.0084	−0.563	576	302	0	0	−150
18	PQ	BGE4	1.0075	−1.678	849	295	0	0	−50
19	PQ	BGN4	1.0086	−1.053	413	149	0	0	−50
20	PQ	AMN4	1.0183	−1.248	127	56	0	0	0
21	PQ	BGC4	1.0099	−0.671	50	182	0	0	0
22	PQ	DYL4	1.0029	−2.029	84	22	0	0	−50
23	PQ	KUT4	1.0249	−4.277	260	108	0	0	−100
24	PQ	QIM4	1.0132	1.222	109	40	0	0	−50
25	PQ	BAB4	1.033	0.041	308	185	0	0	0
26	PQ	KDS4	1.0316	−0.695	213	152	0	0	−50
27	PQ	AMR4	0.9988	−10.44	311	161	0	0	−100
28	PQ	BSR4	1.0052	−10.26	455	145	0	0	0

Table A5. The line data of ISGHV (400 kV).

Line	Bus		Line	R [p.u.]	X [p.u.]	Charging [p.u.]
	From	To				
L1	15	2	2	0.00144	0.01177	0.36439
L2	15	3	1	0.001777	0.016154	0.478634
L3	15	4	1	0.0042	0.03437	1.06426
L4	15	6	1	0.004984	0.04531	1.34251
L5	3	4	1	0.003294	0.02994	0.887224
L6	4	5	1	0.00002	0.0002	0.00584
L7	4	17	2	0.00483	0.04393	1.30165
L8	4	8	1	0.00345	0.03132	0.92808
L9	5	6	1	0.0018	0.01635	0.48447

Table A5. *Cont.*

Line	Bus		Line	R [p.u.]	X [p.u.]	Charging [p.u.]
	From	To				
L10	6	18	1	0.00496	0.04511	1.333667
L11	17	19	1	0.00093	0.00847	0.25099
L12	17	21	1	0.000607	0.005516	0.163436
L13	17	8	1	0.005049	0.045901	1.360021
L14	16	20	2	0.00082	0.00749	0.22181
L15	16	21	1	0.000953	0.00866	0.25682
L16	16	1	1	0.00122	0.01015	0.31897
L17	16	9	1	0.001094	0.009106	0.286176
L18	16	26	1	0.00308	0.02795	0.82827
L19	18	19	1	0.00029	0.00262	0.07763
L20	18	20	1	0.00043	0.00394	0.11674
L21	18	22	1	0.00087	0.00788	0.23348
L22	19	7	2	0.00015	0.00138	0.04086
L23	20	10	1	0.002427	0.022064	0.653744
L24	23	10	1	0.001734	0.01576	0.46696
L25	23	12	1	0.00432	0.03928	1.1639
L26	23	27	1	0.00479	0.04354	1.28998
L27	8	24	1	0.00292	0.02391	0.74035
L28	1	9	1	0.000125	0.001043	0.032791
L29	1	25	2	0.00081	0.00673	0.21165
L30	25	11	1	0.000898	0.00736	0.227
L31	25	26	1	0.00233	0.01935	0.60812
L32	11	26	1	0.002267	0.01857	0.5752
L33	26	12	1	0.00383	0.03485	1.03256
L34	12	14	1	0.00439	0.03993	1.18316
L35	27	13	1	0.0029	0.0264	0.78216
L36	13	14	2	0.00118	0.01076	0.3187
L37	13	28	1	0.000672	0.006107	0.180947
L38	14	28	1	0.000563	0.005122	0.151762
L39	15	2	2	0.00144	0.01177	0.36439

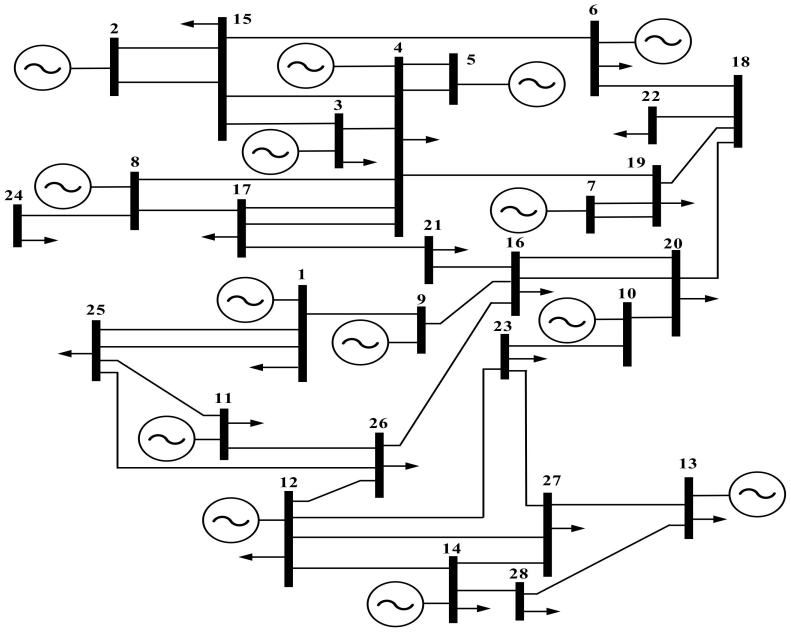

Figure A3. Single-line diagram of ISGHV (400 kV).

References

1. Çelik, D.; Meral, M.E. Current control based power management strategy for distributed power generation system. *Control Eng. Pract.* **2019**, *82*, 72–85. [CrossRef]
2. Carpentier, J. Contribution to the economic dispatch problem. *Bull. La Soc. Fr. Des. Electr.* **1962**, *3*, 431–447.
3. Ebeed, M.; Kamel, S.; Jurado, F. Optimal power flow using recent optimization techniques. In *Classical and Recent Aspects of Power System Optimization*; Elsevier: Amsterdam, The Netherlands, 2018; pp. 157–183. [CrossRef]
4. Abd El-sattar, S.; Kamel, S.; Tostado, M.; Jurado, F. Lightning attachment optimization technique for solving optimal power flow problem. In Proceedings of the 2018 Twentieth International Middle East Power Systems Conference (MEPCON), Cairo, Egypt, 18–20 December 2018; pp. 930–935. [CrossRef]
5. Mirjalili, S.; Mirjalili, S.M.; Lewis, A. Grey wolf optimizer. *Adv. Eng. Softw.* **2014**, *69*, 46–61. [CrossRef]
6. Yang, Y.; Chen, H.; Heidari, A.A.; Gandomi, A.H. Hunger games search: Visions, conception, implementation, deep analysis, perspectives, and towards performance shifts. *Expert Syst. Appl.* **2021**, *177*, 114864. [CrossRef]
7. Heidari, A.A.; Mirjalili, S.; Faris, H.; Aljarah, I.; Mafarja, M.; Chen, H. Harris hawks optimization: Algorithm and applications. *Futur. Gener. Comput. Syst.* **2019**, *97*, 849–872. [CrossRef]
8. Salih, S.Q.; Alsewari, A.A. A new algorithm for normal and large-scale optimization problems: Nomadic People Optimizer. *Neural Comput. Appl.* **2020**, *32*, 10359–10386. [CrossRef]
9. Hashim, F.A.; Houssein, E.H.; Hussain, K.; Mabrouk, M.S.; Al-Atabany, W. Honey Badger Algorithm: New metaheuristic algorithm for solving optimization problems. *Math. Comput. Simul.* **2022**, *192*, 84–110. [CrossRef]
10. Li, S.; Chen, H.; Wang, M.; Heidari, A.A.; Mirjalili, S. Slime mould algorithm: A new method for stochastic optimization. *Futur. Gener. Comput. Syst.* **2020**, *111*, 300–323. [CrossRef]
11. Al-Bahrani, L.; Al-kaabi, M.; Al-saadi, M.; Dumbrava, V. Optimal power flow based on differential evolution optimization technique. *U.P.B. Sci. Bull. Ser. C* **2020**, *82*, 378–388.
12. Al-kaabi, M.; Al-Bahrani, L. Modified Artificial Bee Colony Optimization Technique with Different Objective Function of Constraints Optimal Power Flow. *Int. J. Intell. Eng. Syst.* **2020**, *13*, 378–388. [CrossRef]
13. Al-Bahrani, L.; Al-Kaabi, M.; Al-Hasheme, J. Solving Optimal Power Flow Problem Using Improved Differential Evolution Algorithm. *Int. J. Electr. Electron. Eng. Telecommun.* **2022**, *11*, 146–155. [CrossRef]
14. Al-Kaabi, M.; Al-Bahrani, L.; Dumbrava, V.; Eremia, M. Optimal Power Flow with Four Objective Functions using Improved Differential Evolution Algorithm: Case Study IEEE 57-bus power system. In Proceedings of the 2021 10th International Conference Energy Environ, Bucharest, Romania, 14–15 October 2021; pp. 1–5. [CrossRef]
15. Al-Kaabi, M.; Al Hasheme, J.; Dumbrava, V.; Eremia, M. Application of Harris Hawks Optimization (HHO) Based on Five Single Objective Optimal Power Flow. In Proceedings of the 2022 14th International Conference on Electronics, Computers and Artificial Intelligence (ECAI), Ploesti, Romania, 30 June–1 July 2022; pp. 1–8. [CrossRef]
16. Mohamed, A.; Mohamed, Y.S.; El-Gaafary, A.A.M.; Hemeida, A.M. Optimal power flow using moth swarm algorithm. *Electr. Power Syst. Res.* **2017**, *142*, 190–206. [CrossRef]
17. Abou El-Ela, A.A.; El-Sehiemy, R.; Mouwafi, M.T.; Salman, D. Multiobjective fruit fly optimization algorithm for OPF solution in power system. In Proceedings of the 2018 Twentieth International Middle East Power Systems Conference (MEPCON), Cairo, Egypt, 18–20 December 2018; pp. 254–259. [CrossRef]
18. Datta, R.; Deb, K.; Segev, A. A bi-objective hybrid constrained optimization (HyCon) method using a multi-objective and penalty function approach. In Proceedings of the 2017 IEEE Congress on Evolutionary Computation (CEC), Donostia, Spain, 5–8 June 2017; pp. 317–324. [CrossRef]
19. Davoodi, E.; Babaei, E.; Mohammadi-ivatloo, B. An efficient covexified SDP model for multi-objective optimal power flow. *Int. J. Electr. Power Energy Syst.* **2018**, *102*, 254–264. [CrossRef]
20. Mazza, A.; Chicco, G.; Russo, A. Optimal multi-objective distribution system reconfiguration with multi criteria decision making-based solution ranking and enhanced genetic operators. *Int. J. Electr. Power Energy Syst.* **2014**, *54*, 255–267. [CrossRef]
21. Deb, K. Multi-objective optimisation using evolutionary algorithms: An introduction. In *Multi-Objective Evolutionary Optimisation for Product Design and Manufacturing*; Springer: London, UK, 2011; pp. 3–34. [CrossRef]
22. Hazra, J.; Sinha, A.K. A multi-objective optimal power flow using particle swarm optimization. *Eur. Trans. Electr. Power.* **2011**, *21*, 1028–1045. [CrossRef]
23. Mirjalili, S. Dragonfly algorithm: A new meta-heuristic optimization technique for solving single-objective, discrete, and multi-objective problems. *Neural Comput. Appl.* **2016**, *27*, 1053–1073. [CrossRef]
24. AlRashidi, M.R.; El-Hawary, M.E. Applications of computational intelligence techniques for solving the revived optimal power flow problem. *Electr. Power Syst. Res.* **2009**, *79*, 694–702. [CrossRef]
25. AL-KAABI, M.; Al-Bahrani, L.; Al Hasheme, J. Improved Differential Evolution Algorithm to solve multi-objective of optimal power flow problem. *Arch. Electr. Eng.* **2022**, *71*, 641–657. [CrossRef]
26. Daqaq, F.; Ouassaid, M.; Ellaia, R. A new meta-heuristic programming for multi-objective optimal power flow. *Electr. Eng.* **2021**, *103*, 1217–1237. [CrossRef]
27. El-Sattar, S.A.; Kamel, S.; El Sehiemy, R.A.; Jurado, F.; Yu, J. Single-and multi-objective optimal power flow frameworks using Jaya optimization technique. *Neural Comput. Appl.* **2019**, *31*, 8787–8806. [CrossRef]

28. Kahraman, H.T.; Akbel, M.; Duman, S. Optimization of optimal power flow problem using multi-objective manta ray foraging optimizer. *Appl. Soft Comput.* **2022**, *116*, 108334. [CrossRef]
29. Mirjalili, S.; Jangir, P.; Saremi, S. Multi-objective ant lion optimizer: A multi-objective optimization algorithm for solving engineering problems. *Appl. Intell.* **2017**, *46*, 79–95. [CrossRef]
30. Islam, M.Z.; Wahab, N.I.A.; Veerasamy, V.; Hizam, H.; Mailah, N.F.; Guerrero, J.M.; Mohd Nasir, M.N. A Harris Hawks Optimization Based Single-and Multi-Objective Optimal Power Flow Considering Environmental Emission. *Sustainability* **2020**, *12*, 5248. [CrossRef]
31. Khunkitti, S.; Siritaratiwat, A.; Premrudeepreechacharn, S. Multi-Objective optimal power flow problems based on Slime mould algorithm. *Sustainability* **2021**, *13*, 7448. [CrossRef]
32. Premkumar, M.; Jangir, P.; Sowmya, R.; Elavarasan, R.M. Many-Objective Gradient-Based Optimizer to Solve Optimal Power Flow Problems: Analysis and Validations. *Eng. Appl. Artif. Intell.* **2021**, *106*, 104479. [CrossRef]
33. El-Fergany, A.A.; Hasanien, H.M. Tree-seed algorithm for solving optimal power flow problem in large-scale power systems incorporating validations and comparisons. *Appl. Soft Comput.* **2018**, *64*, 307–316. [CrossRef]
34. IEEE Power Systems Test Case. Available online: http://www.ee.washington.edu/research/pstca/ (accessed on 20 August 2022).
35. Bouchekara, H. Optimal power flow using black-hole-based optimization approach. *Appl. Soft Comput.* **2014**, *24*, 879–888. [CrossRef]
36. Attia, A.; El Sehiemy, R.A.; Hasanien, H.M. Optimal power flow solution in power systems using a novel Sine-Cosine algorithm. *Int. J. Electr. Power Energy Syst.* **2018**, *99*, 331–343. [CrossRef]
37. Nguyen, T.T. A high performance social spider optimization algorithm for optimal power flow solution with single objective optimization. *Energy* **2019**, *171*, 218–240. [CrossRef]
38. Abaci, K.; Yamacli, V. Differential search algorithm for solving multi-objective optimal power flow problem. *Int. J. Electr. Power Energy Syst.* **2016**, *79*, 1–10. [CrossRef]
39. Warid, W.; Hizam, H.; Mariun, N.; Abdul-Wahab, N.I. Optimal power flow using the Jaya algorithm. *Energies* **2016**, *9*, 678. [CrossRef]
40. Roberge, V.; Tarbouchi, M.; Okou, F. Optimal power flow based on parallel metaheuristics for graphics processing units. *Electr. Power Syst. Res.* **2016**, *140*, 344–353. [CrossRef]
41. Biswas, P.P.; Suganthan, P.N.; Mallipeddi, R.; Amaratunga, G.A.J. Optimal power flow solutions using differential evolution algorithm integrated with effective constraint handling techniques. *Eng. Appl. Artif. Intell.* **2018**, *68*, 81–100. [CrossRef]
42. El-Hana Bouchekara, H.R.; Abido, M.A.; Chaib, A.E. Optimal power flow using an improved electromagnetism-like mechanism method. *Electr. Power Compon. Syst.* **2016**, *44*, 434–449. [CrossRef]
43. Taher, M.A.; Kamel, S.; Jurado, F.; Ebeed, M. Modified grasshopper optimization framework for optimal power flow solution. *Electr. Eng.* **2019**, *101*, 121–148. [CrossRef]
44. Kumari, M.S.; Maheswarapu, S. Enhanced genetic algorithm based computation technique for multi-objective optimal power flow solution. *Int. J. Electr. Power Energy Syst.* **2010**, *32*, 736–742. [CrossRef]
45. Warid, W. Optimal power flow using the AMTPG-Jaya algorithm. *Appl. Soft Comput.* **2020**, *91*, 106252. [CrossRef]
46. Abdel-Rahim, A.M.; Shaaban, S.A.; Raglend, I.J. Optimal Power Flow Using Atom Search Optimization. In Proceedings of the 2019 Innovations in Power and Advanced Computing Technologies (i-PACT), Vellore, India, 22–23 March 2019; pp. 1–4. [CrossRef]
47. Surender Reddy, B.P. Efficiency improvements in meta-heuristic algorithms to solve the optimal power flow problem. *Int. J. Elec. Power.* **2016**, *82*, 288–302. [CrossRef]
48. Meng, A.; Zeng, C.; Wang, P.; Chen, D.; Zhou, T.; Zheng, X.; Yin, H. A high-performance crisscross search based grey wolf optimizer for solving optimal power flow problem. *Energy* **2021**, *225*, 120211. [CrossRef]
49. He, X.; Wang, W.; Jiang, J.; Xu, L. An improved artificial bee colony algorithm and its application to multi-objective optimal power flow. *Energies* **2015**, *8*, 2412–2437. [CrossRef]
50. Naderi, E.; Pourakbari-Kasmaei, M.; Cerna, F.V.; Lehtonen, M. A novel hybrid self-adaptive heuristic algorithm to handle single-and multi-objective optimal power flow problems. *Int. J. Electr. Power Energy Syst.* **2021**, *125*, 106492. [CrossRef]
51. Bakirtzis, A.G.; Biskas, P.N.; Zoumas, C.E.; Petridis, V. Optimal power flow by enhanced genetic algorithm. *IEEE Trans. Power Syst.* **2002**, *17*, 229–236. [CrossRef]
52. Lai, L.L.; Ma, J.T.; Yokoyama, R.; Zhao, M. Improved genetic algorithms for optimal power flow under both normal and contingent operation states. *Int. J. Electr. Power Energy Syst.* **1997**, *19*, 287–292. [CrossRef]
53. Niknam, T.; Narimani, M.R.; Aghaei, J.; Azizipanah-Abarghooee, R. Improved particle swarm optimisation for multi-objective optimal power flow considering the cost, loss, emission and voltage stability index. *IET Gener. Transm. Distrib.* **2012**, *6*, 515–527. [CrossRef]
54. Attia, A.; Al-Turki, Y.A.; Abusorrah, A.M. Optimal power flow using adapted genetic algorithm with adjusting population size. *Electr. Power Compon. Syst.* **2012**, *40*, 1285–1299. [CrossRef]
55. Adaryani, M.R.; Karami, A. Artificial bee colony algorithm for solving multi-objective optimal power flow problem. *Int. J. Electr. Power Energy Syst.* **2013**, *53*, 219–230. [CrossRef]
56. Radosavljević, J.; Klimenta, D.; Jevtić, M.; Arsić, N. Optimal Power Flow Using a Hybrid Optimization Algorithm of Particle Swarm Optimization and Gravitational Search Algorithm. *Electr. Power Compon. Syst.* **2015**, *43*, 1958–1970. [CrossRef]

57. Abd El-sattar, S.; Kamel, S.; Ebeed, M.; Jurado, F. An improved version of salp swarm algorithm for solving optimal power flow problem. *Soft Comput.* **2021**, *25*, 4027–4052. [CrossRef]
58. Duman, S. Symbiotic organisms search algorithm for optimal power flow problem based on valve-point effect and prohibited zones. *Neural Comput. Appl.* **2017**, *28*, 3571–3585. [CrossRef]
59. Khan, A.; Hizam, H.; bin Abdul Wahab, N.I.; Lutfi Othman, M. Optimal power flow using hybrid firefly and particle swarm optimization algorithm. *PLoS ONE* **2020**, *15*, e0235668. [CrossRef]
60. Li, S.; Gong, W.; Wang, L.; Yan, X.; Hu, C. Optimal power flow by means of improved adaptive differential evolution. *Energy* **2020**, *198*, 117314. [CrossRef]
61. Khorsandi, A.; Hosseinian, S.H.; Ghazanfari, A. Modified artificial bee colony algorithm based on fuzzy multi-objective technique for optimal power flow problem. *Electr. Power Syst. Res.* **2013**, *95*, 206–213. [CrossRef]
62. Kumar, A.R.; Premalatha, L. Optimal power flow for a deregulated power system using adaptive real coded biogeography-based optimization. *Int. J. Electr. Power Energy Syst.* **2015**, *73*, 393–399. [CrossRef]
63. Chaib, A.E.; Bouchekara, H.; Mehasni, R.; Abido, M.A. Optimal power flow with emission and non-smooth cost functions using backtracking search optimization algorithm. *Int. J. Electr. Power Energy Syst.* **2016**, *81*, 64–77. [CrossRef]
64. Bouchekara, H.; Abido, M.A.; Boucherma, M. Optimal power flow using teaching-learning-based optimization technique. *Electr. Power Syst. Res.* **2014**, *114*, 49–59. [CrossRef]
65. Abido, M.A. Multiobjective optimal power flow using strength Pareto evolutionary algorithm. In Proceedings of the 39th International Universities Power Engineering Conference, Bristol, UK, 6–8 September 2004; pp. 457–461.
66. Abido, M.A.; Al-Ali, N.A. Multi-objective differential evolution for optimal power flow. In Proceedings of the 2009 International Conference on Power Engineering, Energy and Electrical Drives, Lisbon, Portugal, 18–20 March 2009; pp. 101–106. [CrossRef]
67. Saeed, W.; Tawfeeq, L. Voltage Collapse Optimization for the Iraqi Extra High Voltage 400 kV Grid based on Particle Swarm Optimization. *Iraqi J. Electr. Electron. Eng.* **2017**, *13*, 17–31. [CrossRef]
68. Tawfeeq, L. Optimal Power Flow (OPF) with Different Objective Function Based on Modern Heuristic Optimization Techniques. Ph.D. Thesis, University Politehnica of Bucharest, Bucharest, Romania, 2015.
69. Wolpert, D.H.; Macready, W.G. *No Free Lunch Theorems for Search*; Technical Report SFI-TR-95-02-010; Santa Fe Institute: Santa Fe, NM, USA, 1995.
70. Ghasemi, M.; Ghavidel, S.; Ghanbarian, M.M.; Gharibzadeh, M.; Vahed, A.A. Multi-objective optimal power flow considering the cost, emission, voltage deviation and power losses using multi-objective modified imperialist competitive algorithm. *Energy* **2014**, *78*, 276–289. [CrossRef]
71. Shaheen, A.M.; El-Sehiemy, R.A.; Farrag, S.M. Solving multi-objective optimal power flow problem via forced initialised differential evolution algorithm. *IET Gener. Transm. Distrib.* **2016**, *10*, 1634–1647. [CrossRef]
72. Duman, S.; Güvenç, U.; Sönmez, Y.; Yörükeren, N. Optimal power flow using gravitational search algorithm. *Energy Convers. Manag.* **2012**, *59*, 86–95. [CrossRef]
73. Selvakumar, A.I.; Thanushkodi, K. A new particle swarm optimization solution to nonconvex economic dispatch problems. *IEEE Trans. Power Syst.* **2007**, *22*, 42–51. [CrossRef]
74. Roy, P.K.; Paul, C. Optimal power flow using krill herd algorithm. *Int. Trans. Electr. Energy Syst.* **2015**, *25*, 1397–1419. [CrossRef]
75. Vaisakh, K.; Srinivas, L.R. Evolving ant direction differential evolution for OPF with non-smooth cost functions. *Eng. Appl. Artif. Intell.* **2011**, *24*, 426–436. [CrossRef]
76. Shabanpour-Haghighi, A.; Seifi, A.R.; Niknam, T. A modified teaching–learning based optimization for multi-objective optimal power flow problem. *Energy Convers. Manag.* **2014**, *77*, 597–607. [CrossRef]
77. Hsiao, Y.; Chen, C.; Chien, C. Optimal capacitor placement in distribution systems using a combination fuzzy-GA method. *Int. J. Electr. Power Energy Syst.* **2004**, *26*, 501–508. [CrossRef]
78. Ghasemi, M.; Ghavidel, S.; Ghanbarian, M.M.; Gitizadeh, M. Multi-objective optimal electric power planning in the power system using Gaussian bare-bones imperialist competitive algorithm. *Inf. Sci.* **2015**, *294*, 286–304. [CrossRef]
79. Pulluri, H.; Naresh, R.; Sharma, V. A solution network based on stud krill herd algorithm for optimal power flow problems. *Soft Comput.* **2018**, *22*, 159–176. [CrossRef]